Dimer Species in Aqueous Solutions of *m*-Phenylenediamine-*N,N,N',N'*-tetra-acetic Acid (*m*-H_4pdta) with Copper(II) and of Pyridine-2,6-diamine-*N,N,N',N'*-tetra-acetic Acid (2,6-H_4pydta) with Nickel(II). *X*-Ray Crystal Structures of $Na_4[Cu_2(m\text{-pdta})_2]\cdot 18H_2O$, $Na_4[Co_2(m\text{-pdta})_2]\cdot 10H_2O$, and $Na_4[Ni_2(2,6\text{-pydta})_2]\cdot 8H_2O$ †

Alfredo Mederos,* Pedro Gili, Sixto Domínguez, Angel Benítez, Mª Soledad Palacios, Margarita Hernández-Padilla, and Pedro Martín-Zarza
Departamento de Química Inorgánica, Universidad de La Laguna, Tenerife, Canary Islands, Spain
Matías L. Rodríguez and Catalina Ruíz-Pérez
Instituto Universitario de Química Orgánica, Universidad de La Laguna, Tenerife, Canary Islands, Spain
Fernando J. Lahoz and Luis A. Oro
Departamento de Química Inorgánica, Instituto de Ciencia de Materiales de Aragón, Universidad de Zaragoza-Consejo Superior de Investigaciones Científicas, 50009 Zaragoza, Spain
Felipe Brito
Laboratorio de Equilibrios en Solución, Escuela de Química, Facultad de Ciencias, Universidad Central de Venezuela, Caracas, Venezuela
Juan M. Arrieta
Departamento de Química (Inorgánica), Universidad del País Vasco, Apartado 644, Bilbao, Spain
Metaxia Vlassi and Gabriel Germain
Unité de Chimie Physique Moléculaire et de la Cristallographie, Université de Louvain, Place Louis Pasteur 1, 1348 Louvain-la-Neuve, Belgium

Potentiometric investigations in aqueous solution at 25 °C and ionic strength 0.1 mol dm^{-3} KCl have shown that the dimer complex species $[Cu_2L_2]^{4-}$ (ligand H_4L, *m*-phenylenediamine-*N,N,N',N'*-tetra-acetic acid, *m*-H_4pdta) and $[Ni_2L_2]^{4-}$ (ligand H_4L, pyridine-2,6-diamine-*N,N,N',N'*-tetra-acetic acid, 2,6-H_4pydta) are present in significant amounts at $C_M > 2 \times 10^{-3}$ mol dm^{-3}. The formation constants of the monomer and dimer have been determined. The formation of the dimer $[M_2L_2]^{4-}$ from the monomer $[ML]^{2-}$ or $[M(HL)]^-$ is affected by the Jahn–Teller effect (Cu^{II}–*m*-H_4pdta) or by the effect of the withdrawal of electronic density by the pyridine nitrogen of the ring (Ni^{II}–2,6-H_4pydta system). From a concentrated solution with a ligand : metal ratio of 1 : 1 at pH 6, single crystals of the complexes $Na_4[Cu_2(m\text{-pdta})_2]\cdot 18H_2O$, $Na_4[Co_2(m\text{-pdta})_2]\cdot 10H_2O$, and $Na_4[Ni_2(2,6\text{-pydta})_2]\cdot 8H_2O$, respectively, were obtained. *X*-Ray diffraction structural analysis revealed that the dimer molecules are centrosymmetrical (C_i), with each metal atom surrounded by four carboxylic oxygens and two amine nitrogens in a distorted octahedron, the copper(II) complex being the most distorted (Jahn–Teller effect). In the nickel(II) complex the pyridine nitrogen is not bonded. Each sodium is co-ordinated to water molecules and carboxyl groups, being six-co-ordinated in the copper(II) complex and five-co-ordinated in the complexes of Co^{II} and Ni^{II}. The complexes were also characterized by i.r., electronic, and mass spectra, magnetic measurements, and thermogravimetric analysis.

The preparation of co-ordinating agents derived from aromatic diamines is of special interest, since the use of nitrogen atoms for co-ordination to a single cation is directly related to their situation in *ortho*, *meta*, or *para* positions. Thus, in the case of diaminetetramethylenecarboxylic acids, with derivatives of *o*-phenylenediamines, the greater proximity of the nitrogen atoms permits the simultaneous co-ordination of both to the same metal cation, as has been established by the *X*-ray crystallographic determination of the structures of the complexes of *o*-phenylenediamine-*N,N,N',N'*-tetra-acetic acid (*o*-H_4pdta) with Co^{II},[1] Mn^{II},[2] Zn^{II},[3] and Cu^{II}.[4] These results confirmed the studies in aqueous solution of the co-ordinating ability of *o*-H_4pdta acid, 3,4-H_4tdta (3,4-toluenediamine-*N,N,N',N'*-tetra-acetic acid), and H_4cpdta (4-chloro-1,2-phenylenediamine-*N,N,N',N'*-tetra-acetic acid).[5–9] On the other hand, the diaminetetramethylenecarboxylic acid derivatives of *m*- or *p*-phenylenediamines can only co-ordinate one nitrogen atom to any one metal cation. These ligands can therefore co-ordinate in two spheres, as has been proven by the preparation of bimetallic species M_2L in the solid state[10,11] and in studies in aqueous solution[12] for *m*- and *p*-H_4pdta. The formation of species with excess of ligand is also possible, since each iminodiacetic group of the ligand is insufficient co-ordinatively to saturate the central ion, as confirmed by our studies in aqueous solution of the co-ordinating ability of *m*- and *p*-H_4pdta with Cu^{II}[12] and Be^{II}.[13]

In the case of ligands derived from *m*-phenylenediamines, the especial conformation of the ligand with the nitrogen atoms in *meta* positions on the aromatic ring, facilitates the formation of dimer complexes, since the ligands act as a bridge. This has been proven in the case of Schiff bases, by means of *X*-ray diffraction

† *Supplementary data available:* see Instructions for Authors, *J. Chem. Soc., Dalton Trans.*, 1990, Issue 1, pp. xix—xxii.
Non-S.I. units employed: B.M. ≈ 9.27×10^{-24} JT^{-1}; G = 10^{-4} T.

analysis of the structure of the Cu_2 complex of *N,N'-m*-phenylenebis(salicylideneimine),[14] and by mass spectrometry of the Co_2 and Cu_2 complexes of *N,N'-m*-phenylenebis(acetylacetoneimine).[15] In the case of diaminetetramethylenecarboxylic acids evidence was found for the formation in the solid state of complexes with a 2:2 ligand:metal ratio[16] for *m*-H_4pdta and Ni^{II}. A spectrophotometric study[17] in aqueous solution of the system Cu^{II}–*m*-H_4pdta indicated the formation of complex species in the ratio 2:2, but the potentiometric study in aqueous solution of the systems Cu^{II}–*m*-H_4pdta,[12] –2,4-H_4tdta[18] (2,4-toluenediamine-*N,N,N',N'*-tetra-acetic acid), –2,6-H_4tdta[18] (2,6-toluenediamine-*N,N,N',N'*-tetra-acetic acid) and 2,6-H_4pydta[18] (pyridine-2,6-diamine-*N,N,N',N'*-tetra-acetic acid), varying the concentration of the metal cation from 0.5×10^{-3} to 1.5×10^{-3} mol dm^{-3} and analysing the experimental data by means of the NERNST/LETA/GRAFICA version[19] of the LETAGROP program,[20] did not reveal the presence in aqueous solution of significant amounts of 2:2 complexes. However, a similar study of the Co^{II}–[21] and Ni^{II}–*m*-H_4pdta[22] systems, varying the metal concentration from 1×10^{-3} to 2×10^{-3}, or 3×10^{-3} mol dm^{-3} respectively, revealed the presence in aqueous solution of 2:2 complex species. Therefore, the practical absence[12] of the species $[Cu_2L_2]^{4-}$ (neutral ligand = H_4L) at a concentration 1.5×10^{-3} mol dm^{-3} suggests that this species might be formed in aqueous solution at higher concentrations.

In the present work, a study of the conditions for the formation in aqueous solution of dimer species $[M_2L_2]^{4-}$ (neutral ligand = H_4L) has been made for the Cu^{II}–*m*-H_4pdta and Ni^{II}–2,6-H_4pydta systems. Single crystals of the sodium salts of the complexes $[Cu_2L_2]^{4-}$ and $[Ni_2L_2]^{4-}$ were isolated, their structures determined, and their spectroscopic, magnetic, and thermal properties studied. The sodium salt of the species $[Co_2L_2]^{4-}$ (L = *m*-pdta) has also been isolated in the crystalline state and its structure and properties studied.

Experimental

Materials.—The acid *m*-H_4pdta was prepared according to the Blasius and Olbrich method.[23] The monosodium salt of 2,6-H_4pydta acid was prepared according to the literature.[24] Precautions were taken to maintain an inert atmosphere (argon) and prevent the access of light during the preparation and preservation of the ligands and during the study of their solutions, since they are photosensitive and oxidize readily. A carbonate-free sodium hydroxide solution was prepared according to the School of Sillén[25] and standardized against potassium hydrogenphthalate. The metal solutions (in the form of the chloride) were standardized by routine methods. Potassium chloride was prepared by recrystallization of KCl. The compounds HCl, NaOH, KCl, $CuCl_2$, $NiCl_2$, $Cu(NO_3)_2 \cdot 3H_2O$, $Co(NO_3)_2 \cdot 6H_2O$, and $Ni(NO_3)_2 \cdot 6H_2O$ were of analytical grade from Merck.

Potentiometry.—The titrations in aqueous solutions were carried out in an inert argon atmosphere at 25 ± 0.05 °C, I = 0.1 mol dm^{-3} KCl using a Radiometer type PHM-64 potentiometer, a Radiometer G 202 B glass electrode, and K 401 calomel electrode. The cell constants were determined according to the method of Biedermann and Sillén,[26] the liquid-junction potentials being found to be almost negligible within the ranges of $[H^+]$ studied.

Measurements were taken of *m*-H_4pdta in the presence of Cu^{II} at 1:1 ligand:metal ratio and concentrations c_M = 2×10^{-3}, 3×10^{-3}, 4×10^{-3}, 6×10^{-3}, 8×10^{-3}, or 10×10^{-3} mol dm^{-3}, respectively, of the monosodium salt of 2,6-H_4pydta alone at the concentrations $c_L = 1.45 \times 10^{-3}$ (titration with NaOH), 1.54×10^{-3} (NaOH), and 1.70×10^{-3} (HCl) mol dm^{-3}, respectively, and of the monosodium salt of 2,6-H_4pydta in the presence of Ni^{II} at the ligand:metal ratios and concentrations: ratios 3:1 and 1:3, $c_M = 1 \times 10^{-3}$, 2×10^{-3}, and 3×10^{-3} mol dm^{-3}, respectively, and 1:1, $c_M = 1 \times 10^{-3}$, 2×10^{-3}, 3×10^{-3}, 5×10^{-3}, 8×10^{-3}, 10×10^{-3}, and 12×10^{-3} mol dm^{-3}, respectively.

The experimental potentiometric data were analysed by means of the NERNST/LETA/GRAFICA version[19] of the LETAGROP program[20] and by the MINIQUAD program.[27] The ionization constants of *m*-H_4pdta and the stability constants of the other complexes of Cu^{II} with this acid were previously obtained under the same experimental conditions.[12]

The presence of the $[Cu_2(OH)_2]^{2+}$ species, which is the major hydrolytic species of Cu^{II},[28] has been taken into account in the calculations. It was found that, under the experimental conditions used, hydrolysis of Ni^{II} is negligible.

Preparation of the Complexes $Na_4[Cu_2(m\text{-pdta})_2] \cdot 18H_2O$, $Na_4[Co_2(m\text{-pdta})_2] \cdot 10H_2O$, *and* $Na_4[Ni_2(2,6\text{-pydta})_2] \cdot 8H_2O$.—A concentrated solution of the ligand at pH 4 (by addition of NaOH, predominance of the species H_2L^{2-}, Figure 1) was mixed in the ratio 1:1 with a concentrated solution of the appropriate metal nitrate. The final pH was adjusted to 6 by addition of NaOH, this being the most suitable pH for the formation of the complex (predominance of the species $[M_2L_2]^{4-}$, see distribution diagrams of species in Figure 2 for Cu^{II}, ref. 21 for Co^{II}, and Figure 4 for Ni^{II}. Addition of ethanol to the solutions resulted in the precipitation of polycrystalline dust (dark green for Cu^{II}, pinkish violet for Co^{II}, and light green for Ni^{II}). The precipitates were filtered off, washed several times with ethanol, and stored in a desiccator over $CaCl_2$. Crystals suitable for *X*-ray crystallography were grown by liquid–liquid diffusion,[29,30] using water as solvent and ethanol as precipitant.

Crystal analysis: $Na_4[Cu_2(m\text{-pdta})_2] \cdot 18H_2O$ (dark green) (Found: C, 27.70; H, 5.05; Cu, 10.50; N, 4.50. Calc. for $C_{28}H_{60}Cu_2N_4Na_4O_{34}$: C, 27.65; H, 4.95; Cu, 10.45; N, 4.60%); $Na_4[Co_2(m\text{-pdta})_2] \cdot 10H_2O$ (pinkish violet) (Found: C, 30.95; H, 4.40; Co, 10.80; N, 5.20. Calc. for $C_{28}H_{44}Co_2N_4Na_4O_{26}$: C, 31.65; H, 4.15; Co, 11.10; N, 5.25%); $Na_4[Ni_2(2,6\text{-pydta})_2] \cdot 8H_2O$ (green) (Found: C, 30.55; H, 3.60; N, 8.00; Ni, 11.55. Calc. for $C_{26}H_{38}N_6Na_4Ni_2O_{24}$: C, 30.40; H, 3.70; N, 8.20; Ni, 11.40%).

Elemental analyses were performed on a Carlo Erba 1106 automatic analyser. All metals were determined by atomic absorption. The most intense peaks in the mass spectra of the compounds are (*m/z*, relative intensity in %): $Na_4[Cu_2(m\text{-pdta})_2] \cdot 18H_2O$, 386.30(3), 355.25(14), 327.20(9), 257.25(17), and 255.15(24); chemical ionization (methane) (peaks of dimer) 854.18(0.11), 805.69(0.15), and 686.62(0.10%); fast atom bombardment (f.a.b) [glycerol + dimethyl sulphoxide (dmso)] 874(30), 849(18), 782(16), 575(9), and 531(18%); $Na_4[Co_2(m\text{-pdta})_2] \cdot 10H_2O$, 368(3), 255(14), and 241(11); chemical ionization (methane) (peaks of dimer) 866(1), 564(1), and 462(1); $Na_4[Ni_2(2,6\text{-pydta})_2] \cdot 8H_2O$, 280(0.3) and 163(1); f.a.b.- (glycerol + NaCl + diethanolamine) 864(30), 840(37), 783(34), 743(38), 720(70), 653(72), 584(88), 544(100), 523(100), 498(100), and 478(100).

X-*Ray Structure Determinations.*—$Na_4[Cu_2(m\text{-pdta})_2] \cdot 18H_2O$.

Crystal data. $C_{28}H_{60}Cu_2N_4Na_4O_{34}$, M = 1 215.87, triclinic, space group $P\bar{1}$, a = 9.977(1), b = 10.533(1), c = 12.453(1) Å, α = 80.37(1), β = 73.41(2), γ = 88.13(1)°, U = 1 236 $Å^3$ (by least-squares refinement of the 2θ values in the range 20—40° for 16 accurately measured reflections), $F(000)$ = 630, Z = 1, λ(Cu-K_α) = 1.5418 Å, D_m = 1.65 (pycnometric method), D_c = 1.63 g cm^{-3}, μ(Cu-K_α) = 19.45 cm^{-1}, crystal dimensions 0.2 × 0.4 × 0.6 mm.

Data collection and processing. Siemens AED diffractometer

(University of La Laguna), ω—θ scan, graphite-monochromated Cu-K_α radiation; a set of independent reflections with 2θ in the range 3—90° was measured. Of 1 940 independent reflections, 1921 having $I > 3\sigma(I)$ were taking as observed and used in the analysis.

Structure solution and refinement. The structure has been determined by the heavy-atom method (Patterson) and Fourier synthesis.[31] In the course of the isotropic least-squares refinement of the positional parameters of the non-hydrogen atoms an empirical absorption correction was calculated (DIFABS[32]), minimum and maximum corrections being 0.606 and 1.360 respectively. The refinement of the positional and anisotropic thermal parameters for non-hydrogen atoms was carried out by full-matrix least squares (F minimized).

The fractional co-ordinates of the H atoms bound to carbon atoms were generated at the expected positions (C–H 1.00 Å).[33] All these hydrogens were included in the last refinement as fixed isotropic contributions, with isotropic thermal parameters set equal to B_{eq} of the parent atoms. The highest peak on the final Fourier difference syntheses had a density of 0.3 e Å^{-3}. The final discrepancy index $R = 0.063$ (unit weights). Scattering factors were taken from ref. 34.

All calculations were carried out on a Digital Vax 11/780 computer. The final values of the positional co-ordinates are given in Table 4 with the atomic numbering as in Figures 5 and 6. Bond distances, bond angles, torsion angles, and planes are given in Table 5.

$Na_4[Co_2(m\text{-pdta})_2]\cdot 10H_2O$. *Crystal data.* $C_{28}H_{44}Co_2N_4Na_4O_{26}$, $M = 1\,062.49$, triclinic, space group $P\bar{1}$, $a = 9.076\,7(5)$, $b = 9.191\,6(5)$, $c = 13.484\,5(8)$ Å, $\alpha = 93.66(1)$, $\beta = 105.03(1)$, $\gamma = 107.12(1)°$, $U = 1\,026.3(2)$ Å^3 (by least-squares refinement of 2θ values in the range 20—30° of 54 accurately measured reflections), $Z = 1$, λ(Mo-K_α) = 0.710 69 Å, $D_c = 1.719$ g cm^{-3}, $F(000) = 546$, μ(Mo-K_α) = 9.42 cm^{-1}, crystal dimensions 0.315 × 0.357 × 0.551 mm. No absorption correction was applied.

Data collection and processing. Siemens AED-2 diffractometer (University of Zaragoza), ω—2θ mode, graphite-monochromated Mo-K_α radiation; a set of independent reflections with 2θ in the range 3—52° was measured. Of 4 013 independent reflections, 3 866 having $F > 5\sigma(F)$ were considered observed and used in the analysis.

Structure solution and refinement. Patterson and Fourier methods, full-matrix least-squares refinement with anisotropic thermal parameters in the last cycles for all non-hydrogen atoms except the oxygen atom of a disordered water molecule of crystallization, O(34) and O(35), with occupation factors 0.65 and 0.35 respectively. Hydrogen atoms for the *m*-pdta ligand and for two water molecules were localized in Fourier difference maps and refined isotropically. Final R and R' values were 0.036 and 0.041. The SHELX system of computer programs was used.[35] Final atomic co-ordinates for the non-hydrogen atoms are given in Table 6 with the atomic numbering as in Figures 7 and 9(*a*). Bond distances, angles, torsion angles, and planes are given in Table 7.

$Na_4[Ni_2(2,6\text{-pydta})_2]\cdot 8H_2O$. *Crystal data.* $C_{26}H_{38}N_6Na_4Ni_2O_{24}$. $M = 1\,027.7$, triclinic, space group $P\bar{1}$, $a = 9.172(8)$, $b = 9.024(8)$, $c = 13.333(1)$ Å, $\alpha = 104.58(5)$, $\beta = 95.24(5)$, $\gamma = 107.15(5)°$, $U = 1\,004$ Å^3 (by least-squares refinement of the 2θ values in the range 31—39° of 44 accurately measured reflections), $Z = 1$, λ(Mo-K_α) = 0.710 69 Å, $D_c = 1.70$ g cm^{-3}, $F(000) = 528$, μ(Mo-K_α) = 10.8 cm^{-1}, crystal dimensions 0.46 × 0.34 × 0.15 mm.

Data collection and processing. Siemens AED diffractometer (University of Louvain), ω—2θ mode, graphite-monochromated Mo-K_α radiation; a set of independent reflections with 2θ in the range 3—50° was measured. Of 3 530 independent reflections, 3 016 having $I > 2.5\sigma(I)$ were considered observed and used in the analysis. Lorentz, polarization and absorption[36] corrections were applied (maximum and minimum absorption corrections 0.6528 and 0.5030).

Structure solution and refinement. Patterson and Fourier methods, full-matrix least-squares refinement with anisotropic thermal parameters in the last cycles for all non-hydrogen atoms. Hydrogen atoms were introduced in idealized positions and refined isotropically. Final R and R' values 0.051 and 0.059. Maximum Δ/σ in final refinement cycle was 0.03; maximum and minimum electron density in final Fourier difference synthesis 2.5 and −0.5 e Å^{-3}. Scattering factors from ref. 34. Final atomic co-ordinates for the non-hydrogen atoms are given in Table 8 with the atomic numbering as in Figures 8 and 9(*b*). Bond distances, angles, torsion angles, and planes are listed in Table 9.

For the three structures, additional material available from the Cambridge Crystallographic Data Centre comprises H-atom co-ordinates, thermal parameters, and remaining bond distances and angles.

Other Physical Measurements.—Infrared spectra were measured as KBr discs using a Perkin-Elmer 681 spectrophotometer, electronic spectra as diffuse reflectance on a Beckman DU-2 spectrophotometer and in aqueous solution on a Perkin-Elmer 550 S spectrophotometer. Mass spectra obtained by electron impact were recorded on a VG micromass ZAB-2F instrument, the ionization voltage being 70 eV (1.12×10^{-17} J) and the temperature 473 K. Chemical ionization was with methane and f.a.b. was with argon (accelerating voltage was 8 kv, ref. 37).

The magnetic susceptibilities were measured on a Faraday microbalance between 4.2 and 288.5 K for the copper complex. For the cobalt (293 K) and nickel complexes (298 K) the Gouy method was used. The data were corrected for the diamagnetism of the sample holder and for the temperature-independent paramagnetism.

E.s.r. spectra were recorded for the copper complex on a Varian E-109 spectrometer operated at X-band frequency and with diphenylpicrylhydrazyl (dpph) as internal reference.

Thermogravimetric analyses were performed on a Perkin-Elmer TG-2 thermobalance provided with an FD first derivative computer, using a mass of 4 mg and heating velocity of 10 °C min^{-1} in a nitrogen atmosphere.

Results and Discussion

Aqueous Solution Studies.—(*a*) Cu^{II}–*m*-pdta. Since the dimeric species $[Cu_2L_2]^{4-}$ might be formed[12] at concentrations of Cu^{II} above 1.5×10^{-3} mol dm^{-3}, three potentiometric titrations were performed at the ligand:metal ratio of 1:1 and copper(II) concentrations of 2×10^{-3}, 3×10^{-3}, and 4×10^{-3} mol dm^{-3}, respectively. In accord with equilibrium (1), the

$$pH^+ + qCu^{2+} + rH_4L \overset{\beta_{pqr}}{\rightleftharpoons} [H_pCu_q(H_4L)_r]^{(p+2q)+} \quad (1)$$

constants β_{-411} (complex $[CuL]^{2-}$) and β_{-822} (complex $[Cu_2L_2]^{4-}$) were varied, maintaining invariable K_w, the ionization constants of *m*-H_4pdta acid[12] [distribution diagram, Figure 1(*a*)], the formation constants of the other complexes of Cu^{II} with *m*-H_4pdta[12,18] (Table 3), and the formation constant of the hydrolytic species[29] $[Cu_2(OH)_2]^{2+}$. The analysis of the experimental data was performed by means of the NERNST/LETA/GRAFICA version[19] of the LETAGROP program [minimizing the function $U = \Sigma (Z_{expl.} - Z_{calc.})^2$, Z being the average number of dissociated protons by atom q of metal].[20] The best fits are given in Table 1. The constant β_{-822} is rather inaccurate, since the dimer species $[Cu_2L_2]^{4-}$ are present in low concentration in aqueous solution, as can also be seen from the distribution diagram in Figure 2(*a*), $c_M = 2 \times 10^{-3}$ mol dm^{-3}.

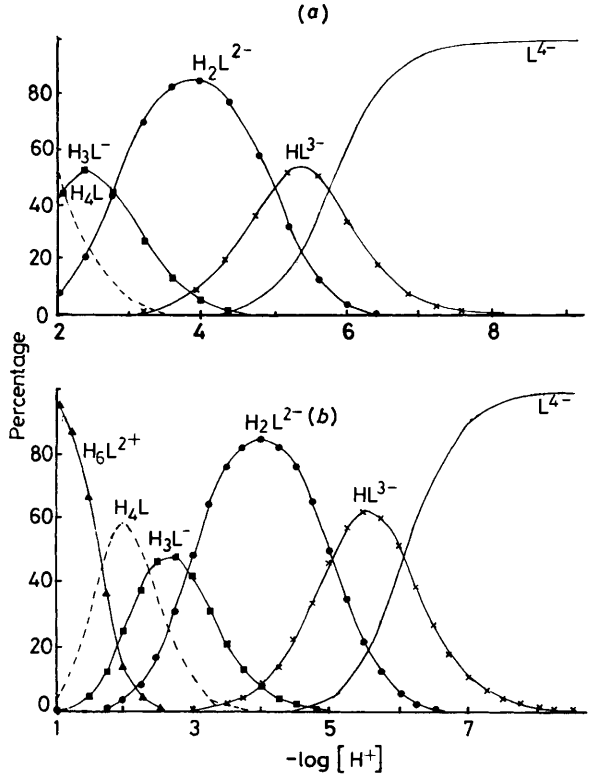

Figure 1. Species distribution as a function of $-\log[H^+]$: (*a*) *m*-H_4pdta, calculated from the values of pK_2 given in ref. 12; (*b*) 2,6-H_4pydta, calculated from the values of pK_2 given in Table 2

Table 1. Formation constants of the complexes $[CuL]^{2-}$ and $[Cu_2L_2]^{4-}$ of *m*-H_4pdta(H_4L) (25 °C; I = 0.1 mol dm^{-3} KCl)

(*a*) LETAGROP program

pqr	$-\log \beta_{pqr}$	Equilibrium	log *K*
−411	7.17 ± 0.05	(2)	8.47 ± 0.05
−822	13.44 (> 12.55)	(3)	17.84 ± 0.92

Three titrations (ratio 1:1), $c = 2 \times 10^{-3}$, 3×10^{-3}, and 4×10^{-3} mol dm^{-3}, respectively; 122 points; $-\log[H^+]$ range 2.53—6.58; standard deviation [$\sigma(Z)$] 0.036.

(*b*) MINIQUAD program

Equilibrium	log *K*
(2) $Cu^{2+} + L^{4-} \rightleftharpoons [CuL]^{2-}$	8.28 ± 0.07
(3) $2Cu^{2+} + 2L^{4-} \rightleftharpoons [Cu_2L_2]^{4-}$	17.92 ± 0.31

Six titrations (ratio 1:1), $c = 2 \times 10^{-3}$, 3×10^{-3}, 4×10^{-3}, 6×10^{-3}, 8×10^{-3}, and 10×10^{-3} mol dm^{-3}, respectively; 128 points; $-\log[H^+]$ range 2.50—4.70; *R* factor 0.011; standard deviation 6.223×10^{-5}.

In order to obtain more accurately the formation constant of the complex $[Cu_2L_2]^{4-}$, three other potentiometric titrations with a ligand:metal ratio of 1:1 and at higher concentrations of Cu^{II}, 6×10^{-3}, 8×10^{-3}, and 10×10^{-3} mol dm^{-3}, respectively, were performed.

Maintaining invariable the values of the formation constants of the same species indicated above, the analysis of the experimental data was carried out by use of the MINIQUAD program.[27] The formation constants of the monomeric species [equilibrium (2), Table 1] and the dimer species [equilibrium (3), Table 1] were changed, and a more accurate value obtained, as expected, for the formation constant of the species $[Cu_2L_2]^{4-}$. The final fit is made with the six potentiometric titrations (from

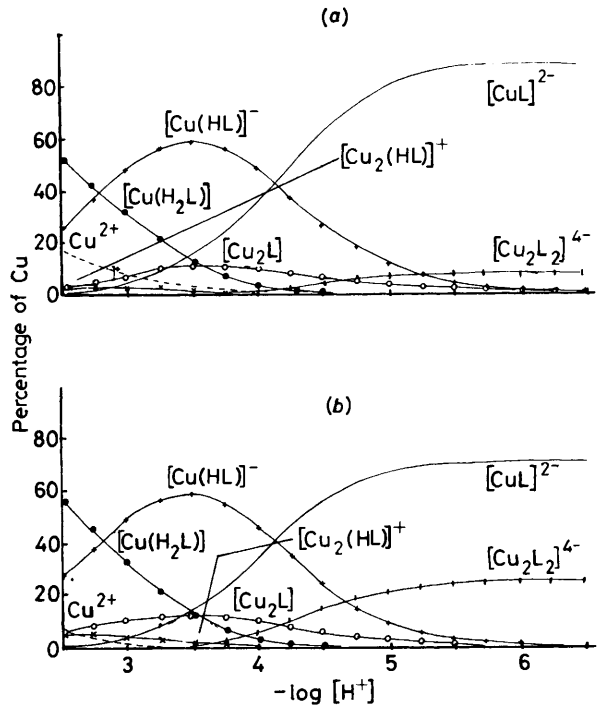

Figure 2. Species distribution as a function of $-\log[H^+]$ for the Cu^{II}–*m*-H_4pdta system (ligand:metal ratio 1:1), $c_M = 2 \times 10^{-3}$ (*a*) and 10×10^{-3} mol dm^{-3} (*b*). Calculated from the values of log *K* given in Table 3

2×10^{-3} to 10×10^{-3} mol dm^{-3}) and the values given in Table 1 were obtained.

The formation constants of the eleven complex species formed by Cu^{II} and *m*-H_4pdta acid are summarized in Table 3, and compared with the corresponding formation constants of Ni^{II}[22] (which does not form significant amounts of complex species with excess of ligand in the ligand:metal ratio 2:1) and Co^{II}[21] (which does not form significant amounts of complex species with excess of ligand and with excess of metal in the ligand:metal ratios 2:1 and 1:2, respectively). Table 3 also includes, together with those of other equilibria, the constants corresponding to the dimerization equilibria (17) and (22).

For log *K* of the monomer complex $[ML]^{2-}$ ($Cu^{II} \gg Ni^{II} > Co^{II}$) and log *K* of the dimer $[M_2L_2]^{4-}$ ($Cu^{II} > Ni^{II} > Co^{II}$), the Irving and Williams order of complexation is fulfilled (Table 3). However, such is not the case for the dimerization constant [equilibrium (17)], where the order is $Ni^{II} > Co^{II} > Cu^{II}$. In the monomeric complexes, *m*-pdta behaves as a tridentate ligand, bonding through an iminodiacetate group to the metal cation. The remainder of the co-ordination is completed by molecules of solvent.[11,38] The Irving–Williams order is related to the ligand-field stabilization energies, and in particular the strength of the M–N bond. However, the dimerization process is easier for Ni^{II} and Co^{II} than for Cu^{II}. As can be readily observed from the crystal structures of dimeric species of Co^{II} (Figure 7) and Ni^{II} (Figure 8), the co-ordination octahedra of these cations are more regular than those corresponding of Cu^{II} (Figure 5).

In other words, dimerization in which the metal cation is bonded to two iminodiacetate groups of different ligands, and for the d^9 ion, is affected by the Jahn–Teller effect, this being the reason for the more difficult dimerization of the copper(II) complexes. For the crystalline dimers of Co^{II} (Table 7, Co–N 2.281 and 2.297 Å, respectively) and Ni^{II} (Table 9, Ni–N 2.215 and 2.237 Å, respectively), M–N bond distances corresponding to iminodiacetate groups of different ligands are practically equal. This is not the case in the complex of Cu^{II} (Figure 5,

Table 2. Ionization constants of 2,6-H_4pydta and formation constants of its complexes with nickel(II) (25 °C, I = 0.1 mol dm^{-3} KCl)

Acid: (*a*) LETAGROP program

pr	$-\log \beta_{pr}$	Equilibrium	pK_i
11	−2.121 ± 0.147	(5) $H_4L \rightleftharpoons H_3L^- + H^+$	2.12
−11	2.920 ± 0.024	(6) $H_3L^- \rightleftharpoons H_2L^{2-} + H^+$	2.92
−21	7.945 ± 0.024	(7) $H_2L^{2-} \rightleftharpoons HL^{3-} + H^+$	5.03
−31	14.012 ± 0.025	(8) $HL^{3-} \rightleftharpoons L^{4-} + H^+$	6.07

One titration (NaOH), c = 1.45 × 10^{-3} mol dm^{-3}; 33 points; −log [H$^+$] range 3.10—8.27; standard deviation [σ(Z)] 0.004.

(*b*) MINIQUAD program

61	19.785 ± 0.011	(11) $H_6L^{2+} \rightleftharpoons H_4L + 2H^+$	3.35
41	16.434 ± 0.010	(5)	2.38
31	14.054 ± 0.009	(6)	2.94
21	11.112 ± 0.005	(7)	5.04
11	6.072 ± 0.004	(8)	6.07

Three titrations, c = 1.45 × 10^{-3} and 1.54 × 10^{-3} mol dm^{-3} (NaOH), 1.7 × 10^{-3} mol dm^{-3} (HCl); 107 points; −log [H$^+$] range 1.70—8.50; R 0.001; standard deviation 7.059 × 10^{-6}.

Complexes: (*a*) LETAGROP program

pqr	$-\log \beta_{pqr}$	Equilibrium	log K
−211	4.76 ± 0.06	(13) $Ni^{2+} + HL^{3-} \rightleftharpoons [Ni(HL)]^-$	3.19 ± 0.08
−311	9.43 ± 0.03	(14) $Ni^{2+} + L^{4-} \rightleftharpoons [NiL]^{2-}$	4.58 ± 0.06
−622	17.46(>16.77)	(15) $2Ni^{2+} + 2L^{4-} \rightleftharpoons [Ni_2L_2]^{4-}$	10.56 ± 0.66

Six titrations (ligand/metal ratios 1:1 and 1:3), c_M = 1 × 10^{-3}, 2 × 10^{-3}, and 3 × 10^{-3} mol dm^{-3}, respectively; 86 points; −log [H$^+$] range 2.92—8.69; standard deviation [σ(Z)] 0.024.

(*b*) MINIQUAD program

111	9.32 ± 0.03	(13)	3.25 ± 0.06
011	4.59 ± 0.04	(14)	4.59 ± 0.04
022	10.85 ± 0.22	(15)	10.85 ± 0.22

Seven titrations (ratio 1:1), c_M = 1 × 10^{-3}, 2 × 10^{-3}, 3 × 10^{-3}, 5 × 10^{-3}, 8 × 10^{-3}, 10 × 10^{-3}, and 12 × 10^{-3} mol dm^{-3}, respectively; 198 points; −log [H$^+$] range 2.70—9.00; R 0.014; standard deviation 1.197 × 10^{-5}.

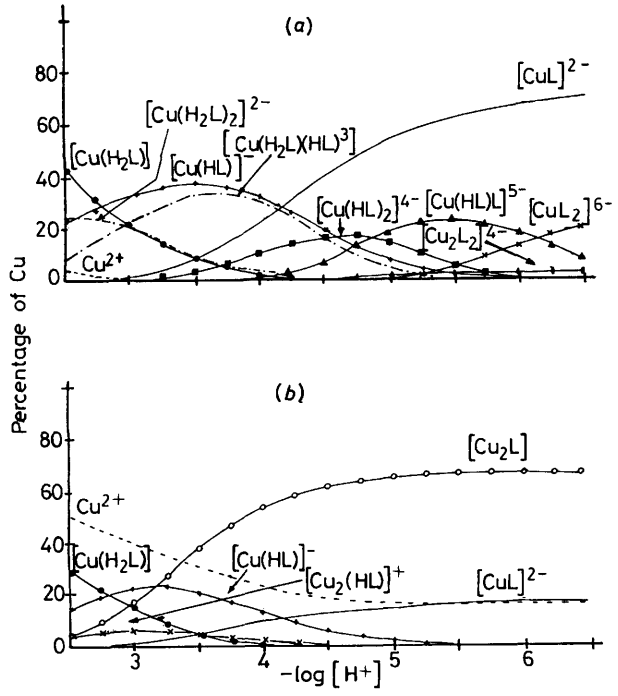

Figure 3. Species distribution as a function of −log[H$^+$] for the Cu^{II}–*m*-H_4pdta system at c_M = 2 × 10^{-3} mol dm^{-3}. Ligand:metal ratio: 2:1 (*a*) and 1:2 (*b*). Calculated from the values of log K given in Table 3

Table 5), where a shorter Cu–N bond (2.075 Å), corresponding to the iminodiacetate group initially coupled to the cation, is followed by a longer Cu–N bond (2.509 Å) corresponding to the iminodiacetate group of the other ligand. The influence of the Jahn–Teller effect must be taken into account whether the dimerization is verified from the non-protonated complex $[CuL]^{2-}$ [equilibrium (17)], or from the monoprotonated complex $[Cu(HL)]^-$ [equilibrium (22)]. In the case of *m*-pdta, the protons of the species H_2L^{2-} and HL^{3-} are betainic protons[39,40] [distribution diagram, Figure 1(*a*)]. The values of pK_i for the species $[M(HL)]^-$ [Table 3, equilibrium (21)] are consistent with a betainic proton bonded to an iminodiacetate group.[39,40] If these values are compared with the pK_i corresponding to equilibrium (22) (Table 3), an increase is observed in the acidity corresponding to the formation of the dimer species $[M_2L_2]^{4-}$, but this increase follows the order $Cu^{II} \ll Co^{II} < Ni^{II}$. The betainic proton of the species $[M(HL)]^-$ is displaced with more difficulty in the case of Cu^{II} to form the dimer species $[M_2L_2]^{4-}$, due to the Jahn–Teller effect of the d^9 cation, and the acidity is weaker.

The species distribution diagrams as a function of −log[H$^+$] for Cu^{II} (Figure 2, ratio 1:1) indicate that the percentage of the dimer species must increase with the concentration since equilibrium (17) is displaced to the right (Table 3): at a concentration 10 × 10^{-3} mol dm^{-3} [Figure 2(*b*)], the proportion represented by the complex $[CuL]^{2-}$ is 70% and that of $[Cu_2L_2]^{4-}$, 27%; these values are 61 and 36%, respectively, at 20 × 10^{-3} mol dm^{-3}. Figure 3(*a*) shows that at the ligand:metal ratio 2:1 the species $[CuL]^{2-}$ competes at pH 6 with the species formed with excess of ligand, $[Cu(HL)L]^{5-}$ and $[CuL_2]^{6-}$; at 2 × 10^{-3} mol dm^{-3}, the species $[Cu_2L_2]^{4-}$ represents only 4%. In Figure 3(*b*) it can be seen that at the ligand:metal ratio 1:2, $[CuL]^{2-}$ competes at pH 6 with the bimetallic species $[Cu_2L]$; at the same concentration, $[Cu_2L_2]^{4-}$ is practically non-

Table 3. Formation constants (log K) of the complexes of *m*-pdta with copper(II), nickel(II), and cobalt(II) and of 2,6-pydta with nickel(II) (25 °C, I = 0.1 mol dm^{-3} KCl)

Species	*m*-pdta				2,6-pydta
	Cu^{II}		Ni^{II}	Co^{II}	Ni^{II}
$[M(H_2L)]$	4.47[a]		1.70[b]	2.06[c]	
$[M(HL)]^-$	6.65		3.98	3.33	3.25[d]
$[ML]^{2-}$	8.22	8.28[d]	5.26	5.02	4.59
$[M_2L_2]^{4-}$		17.92	14.38	12.93	10.85
$[M(H_2L)_2]^{2-}$	7.62				
$[M(H_2L)(HL)]^{3-}$	9.65				
$[M(HL)L]^{5-}$	10.81				
$[ML_2]^{6-}$	10.65				
$[M_2(HL)]^+$	8.82				
$[M_2L]$	12.07		7.86		
Equilibrium					
(17) $2[ML]^{2-} \rightleftharpoons [M_2L_2]^{4-}$		1.36	3.86	2.89	1.67
(18) $[ML]^{2-} + M^{2+} \rightleftharpoons [M_2L]$	3.85		2.58		
Equilibrium (pK_i values)					
(19) $H_2L^{2-} + M^{2+} \rightleftharpoons [M(HL)]^- + H^+$	−1.65		1.02	1.67	1.79
(20) $[M(H_2L)] \rightleftharpoons [M(HL)]^- + H^+$	2.82		2.73	3.73	
(21) $[M(HL)]^- \rightleftharpoons [ML]^{2-} + H^+$	4.18		4.47	4.06	4.73
(22) $2[M(HL)]^- \rightleftharpoons [M_2L_2]^{4-} + 2H^+$		7.00	5.08	5.23	7.79
(23) $H_2L^{2-} + M^{2+} \rightleftharpoons [ML]^{2+} + 2H^+$		2.47	5.49	5.73	6.52
(24) $2H_2L^{2-} + 2M^{2+} \rightleftharpoons [M_2L_2]^{4-} + 4H^+$		3.58	7.12	8.57	11.37

[a] From refs. 12 and 18. [b] From ref. 22. [c] From ref. 21. [d] This work.

existent (0.25% at pH 6). Figure 2 indicates that a concentrated solution with a ligand:metal ratio of 1:1 at pH 6 is suitable for the synthesis of crystalline salts of the dimeric complex species $[Cu_2L_2]^{4-}$.

(*b*) Ni^{II}–2,6-pydta *Ionization constants of the acid.* From the values obtained for the constants β_{pr} corresponding to equilibrium (4) (LETAGROP program[19,20]) the ionization

$$pH^+ + rH_3L^- \rightleftharpoons [H_p(H_3L)_r]^{(p-r)+} \quad (4)$$

constants of the acid K_i given in Table 2, could readily be determined (ligand H_3L^-, monosodium salt of 2,6-H_4pydta acid). Equilibrium (5), Table 2, is not well defined, being a titration with NaOH. A further titration was carried out with NaOH and another with HCl. The experimental results were then analysed by means of the MINIQUAD program,[27] in accordance with equilibrium (9).

$$pH^+ + rL^{4-} \overset{\beta_{pr}}{\rightleftharpoons} [H_pL_r]^{(p-4r)+} \quad (9)$$

The values of $-\log \beta_{pr}$ and the corresponding pK_i are given in Table 2. The protonation constant β_{51} is rejected, but β_{61} is well defined, possibly because the protonation equilibria (10) are simultaneous, giving place to the overall equilibrium (11).

$$H^+ + H_4L \rightleftharpoons H_5L^+$$

$$H^+ + H_5L^+ \rightleftharpoons H_6L^{2+} \quad (10)$$

$$2H^+ + H_4L \rightleftharpoons H_6L^{2+} \quad (11)$$

The values of pK_i obtained from the monosodium salt of 2,6-H_4pydta acid are more accurate than those obtained from 2,6-H_4pydta,[18] since the salt is more easily obtained with a greater degree of purity.[24] The values of pK_3 and pK_4 correspond to fundamentally betainic protons.[24] The non-protonation of the pyridinic nitrogen atom in 2,6-H_4pydta is exceptional.[24] The distribution diagram of the species as a function of $-\log[H^+]$ is presented in Figure 1(*b*). The diprotonated H_2L^{2-} species, with the betainic protons, has the largest field of existence and is the most important at pH 4.

Stability constants of the complexes formed. Six potentiometric titrations (ligand:metal ratios 1:1 and 1:3) at nickel(II) concentrations of 1×10^{-3}, 2×10^{-3}, and 3×10^{-3} mol dm^{-3}, respectively, were analysed by means of the LETAGROP program.[19,20] The model that best fits the experimental results corresponds to the complex species in Table 2. From the values obtained for the constants β_{pqr} corresponding to equilibrium (12) the stability constants K could readily be determined.

$$pH^+ + qNi^{2+} + rH_3L^- \rightleftharpoons [H_pNi_q(H_3L)_r]^{(p+2q-r)+} \quad (12)$$

Although models were tested that included the possible presence of complex species with an excess of metal and with an excess of ligand (ligand:metal ratio 3:1, $c_M = 1 \times 10^{-3}$, 2×10^{-3}, and 3×10^{-3} mol dm^{-3}, respectively), the results indicate that they are not present in significant amounts.

The constant β_{-622} is rather inaccurate, since the dimeric species $[Ni_2L_2]^{4-}$ is present in low concentration in aqueous solution, as can be seen from the species distribution diagram in Figure 4(*a*), $c_M = 2 \times 10^{-3}$ mol dm^{-3}. In order to obtain more accurately the formation constant of the complex $[Ni_2L_2]^{4-}$, four other potentiometric titrations with a ligand:metal ratio of 1:1 and at higher concentrations of Ni^{II} (Table 2) were performed. The analysis of the experimental data (seven potentiometric titrations, from 1×10^{-3} to 12×10^{-3} mol dm^{-3}) was carried out by use of the MINIQUAD program.[27] From the values obtained for the constants β_{pqr} corresponding to equilibrium (16) the stability constants K could readily be determined (Table 2).

$$pH^+ + qNi^{2+} + rL^{4-} \rightleftharpoons [H_pNi_qL_r]^{(p+2q-4r)+} \quad (16)$$

The formation constants of the complex species formed by

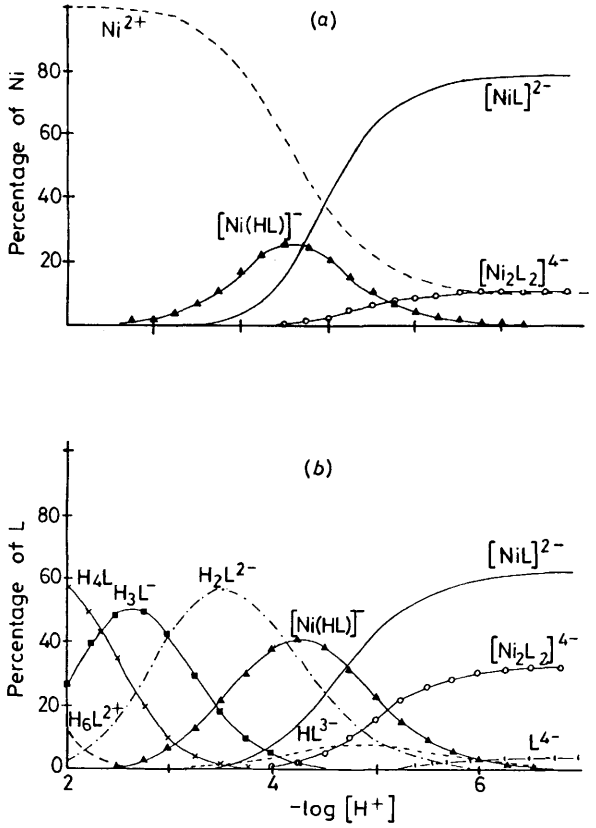

Figure 4. Species distribution as a function of $-\log[H^+]$ for the Ni^{II}–2,6-H_4pydta system (ligand:metal ratio 1:1): (*a*) % Ni, $c_M = 2 \times 10^{-3}$ mol dm^{-3}; (*b*) % L, $c_M = 10 \times 10^{-3}$ mol dm^{-3}. Calculated from the values of pK_i and log *K* given in Table 2

Ni^{II} and 2,6-H_4pydta acid are also summarized in Table 3 and compared with the corresponding formation constants of the Ni^{II}–*m*-H_4pdta system.[22] The dimer $[Ni_2L_2]^{4-}$ has been identified for the first time in potentiometric studies in aqueous solution. Figure 4(*a*) ($c_M = 2 \times 10^{-3}$ mol dm^{-3}) and (*b*) ($c_M = 10 \times 10^{-3}$ mol dm^{-3}) indicate that an increase in concentration facilitates the formation of the dimer species $[Ni_2L_2]^{4-}$ with respect to the monomer $[NiL]^{2-}$, as expected [equilibrium (17)]: at pH 6 the amount of dimer is 9.0 and 30.5% at $c_M = 2 \times 10^{-3}$ and 10×10^{-3} mol dm^{-3}, respectively. The diagrams also indicate that the species $[Ni(HL)]^-$ is transformed into $[NiL]^{2-}$ [equilibrium (21)] or $[Ni_2L_2]^{4-}$ [equilibrium (22)], although Figure 4(*b*) reveals that the complexes $[NiL]^{2-}$ and $[Ni_2L_2]^{4-}$ are mainly formed in accordance with equilibria (23) and (24). Figure 4 also indicates that a concentrated solution with a ligand:metal ratio 1:1 at pH 6 is suitable for the synthesis of crystalline salts of the dimer complexes $[Ni_2L_2]^{4-}$.

For the nickel(II) complexes, Table 3 [equilibria (17) and (22)] indicates that the dimerization process is easier for *m*-H_4pdta than for 2,6-H_4pydta. In general, the values of log *K* (Table 3), which follow the order 2,6-pydta < *m*-pdta, can be explained by considering the lower basicity of the N atoms in the iminodiacetate groups of 2,6-pydta due to the effect of the withdrawal of electron density by the pyridine N of the ring; Ni^{II} is not bonded to this atom (Figure 8).

Crystal Structures.—$Na_4[Cu_2(m\text{-pdta})_2]\cdot 18H_2O$. Crystals of this compound consist of sodium cations, binuclear copper(II) anions, and water of crystallization. Figure 5 displays the dimeric anion $[Cu_2(m\text{-pdta})_2]^{4-}$ showing the atomic numbering scheme and Figure 6 exhibits a schematic representation of the co-ordination spheres for both types of sodium atoms. Atomic co-ordinates are given in Table 4, selected bond distances and angles in Table 5.

The dimeric anion is formed by two copper atoms bridged by two *m*-phenylenediaminetetra-acetate ligands. Each iminodiacetate group of the ligand is bonded to a different metal centre through two carboxylic oxygen atoms and the corresponding nitrogen. The asymmetric unit is formed by one metal atom, the iminodiacetate group of one ligand, and the iminodiacetate group of the other (see Figure 5). The whole anion has a crystallographic C_i symmetry, the Cu ··· Cu separation being 6.931(8) Å.

The geometry about the copper(II) can be described as essentially highly distorted octahedral. The equatorial plane is made up of atoms N(5), O(9), O(16′), and O(24′) and is tetrahedrally distorted with the deviations shown in Table 5. In this plane the co-ordination bond lengths vary for Cu–O from 1.936(7) to 1.969(7) Å, while the Cu–N bond length is 2.075(8) Å. The Cu–O(1) bond distance is 2.293(7) Å while the axial Cu–N(20′) bond distance is 2.509(8) Å. The angle O(1)–Cu–N(20′) between the axial bonds is 154.2(2)°. The angles O(16′)–Cu–N(20′) and O(24′)–Cu–N(20′) are 77.3(3) and 72.8(3)° respectively, while O(9)–Cu–N(20′) and N(5)–Cu–N(20′) are 104.1(3) and 120.4(3)° respectively. These angles together with the axial bond lengths give an impression of the degree of distortion of the octahedron.

The C–O distances of the carboxylate groups correspond to symmetrical groups, with the exception of C(17′)–O(16′) and C(17′)–O(18), 1.290(14) and 1.212(13) Å respectively. In this case, O(16′) is bonded to a copper and a sodium, while O(18′) is bonded to a sodium cation and to a molecule of H_2O (Figure 6). This asymmetry is similar to that found for a carboxylate group of the complex $Na_2[Co(H_2O)_6][Co(o\text{-pdta})]_2\cdot 4H_2O$.[1]

Each sodium is six-co-ordinated to oxygen atoms of water molecules and carboxylate groups (Figure 6), in a distorted octahedron. The Na–O distances are of the order of those found by McCandlish *et al.*[1] for the complex $Na_2[Co(H_2O)_6][Co(o\text{-pdta})]_2\cdot 4H_2O$. The remainder of the molecules of water are present as reticular water [OW(6), OW(8), and OW(9)]; OW(6) and OW(8) are hydrogen bonded [OW(6) ··· OW(8) 2.753(16) Å].

It is interesting to compare this behaviour with that of similar complexes. Thus, in the complex $[Cu(H_2edta)]\cdot H_2O$, the ligand (H_4edta = ethylenediamine-*N*,*N*,*N*′,*N*′-tetra-acetic acid) is quinquedentate,[41] the molecule of water occupying the sixth co-ordination site. The tetragonal bonds Cu–N and Cu–O are 2.291 and 2.467 Å, respectively, while the four equatorial bonds are of the same order, approximately 2 Å. The tetragonality, $T = R_S/R_L = 0.90$ (where R_S is the in-plane bond length and R_L the out-of-plane bond length), was calculated for the Cu–N bonds, and it was supposed that the co-ordination of the metal tends more towards a square-based pyramid than a strictly tetragonal one. For the complex described here, the tetragonality for the bonds Cu–O and Cu–N is 0.849 and 0.827, respectively. These values suggest a similar distortion in the axial and equatorial directions; thus the co-ordination of the copper is strongly distorted.

In the complex $Na_2[Cu(o\text{-pdta})]\cdot 4H_2O$, the ligand is sexidentate,[4] the co-ordination geometry of the copper proving to be very distorted with respect to the symmetry O_h, deviating towards a prism due to the planarity of the *o*-phenylenediamine-*N*,*N*,*N*′,*N*′ chelate ring. In this case, the two Cu–N bond lengths are 2.253(1) and 2.266(2) Å, approximately 0.217 Å longer than in the complex $[Mn(edta)Cu(H_2O)_4]_nZn\cdot H_2O$.[42] N. Nakasuka *et al.*[4] attribute this difference to the lower basicity of the aromatic nitrogens with respect to the aliphatic one and to the geometric restriction imposed by the planar configuration of the phenylenediamine ring.

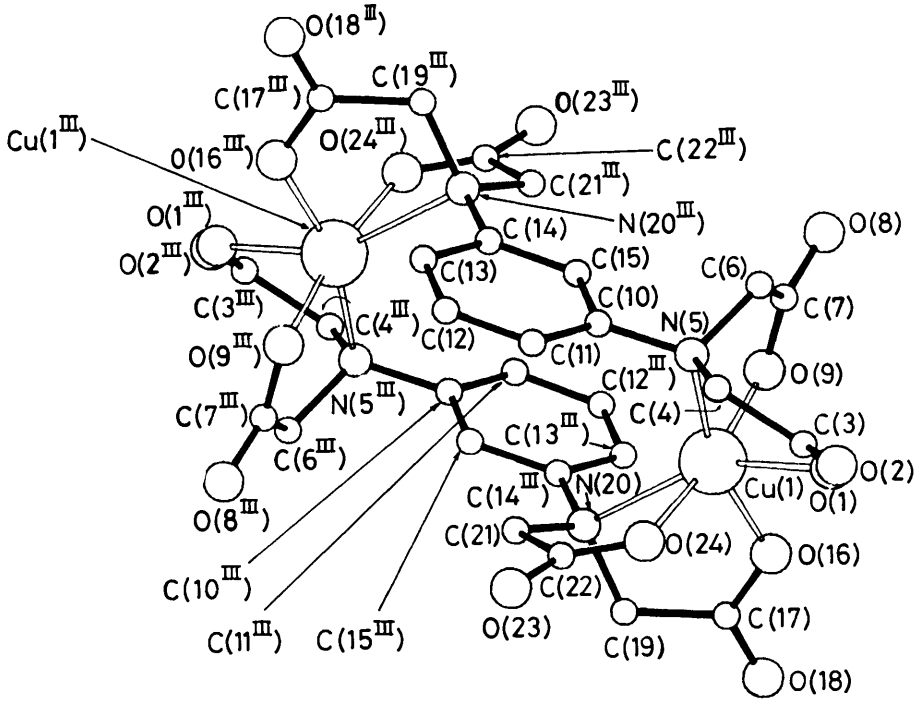

Figure 5. View of the molecular structure of the anionic complex $[Cu_2(m\text{-pdta})_2]^{4-}$ with the atomic numbering scheme used in Table 4. Atoms with superscript III are related by the transformation III $-x, -y, 1-z$

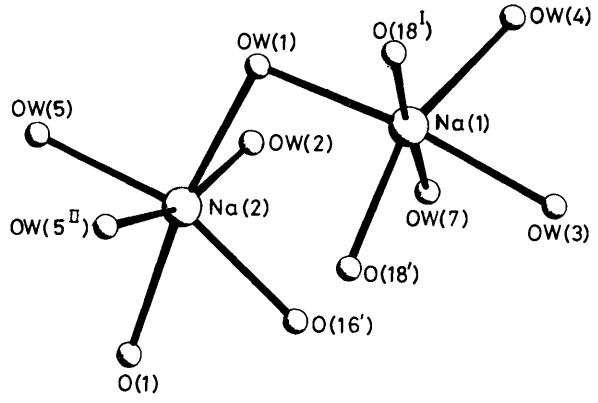

Figure 6. Co-ordination geometry of the sodium atoms in $Na_4[Cu_2(m\text{-pdta})_2]\cdot 18H_2O$ with the labelling scheme given in Table 5

In the monomeric complex $H_2[Zn(o\text{-pdta})(H_2O)]\cdot H_2O$ an oxygen of a co-ordinated carboxylate is thus substituted by a molecule of water and the co-ordination presented is of octahedral symmetry.[3]

Unlike H_4edta and o-H_4pdta acids which have a single co-ordination sphere, the ligands being potentially sexidentate, m-H_4pdta, because of the special conformation of its nitrogen atoms, presents two co-ordination spheres, one corresponding to each iminodiacetic acid group. The formation of the dimeric species $[Cu_2(m\text{-pdta})_2]^{4-}$ implies the utilization by the metal cation of two iminodiacetate groups of different ligands. For this reason m-pdta maintains the distorted octahedron in the dimer.

$Na_4[Co_2(m\text{-pdta})_2]\cdot 10H_2O$. Crystals of this compound consist of sodium cations, binuclear cobalt anions, and water of crystallization. Figure 7 displays the dimeric anion $[Co_2(m\text{-pdta})_2]^{4-}$ showing the atomic numbering scheme, and Figure 9(*a*) a schematic representation of the co-ordination spheres for both types of sodium atoms. Atomic co-ordinates are given in Table 6, selected bond distances and angles in Table 7. The dimeric anion $[Co_2(m\text{-pdta})_2]^{4-}$ is analogous to the copper dimeric anion.

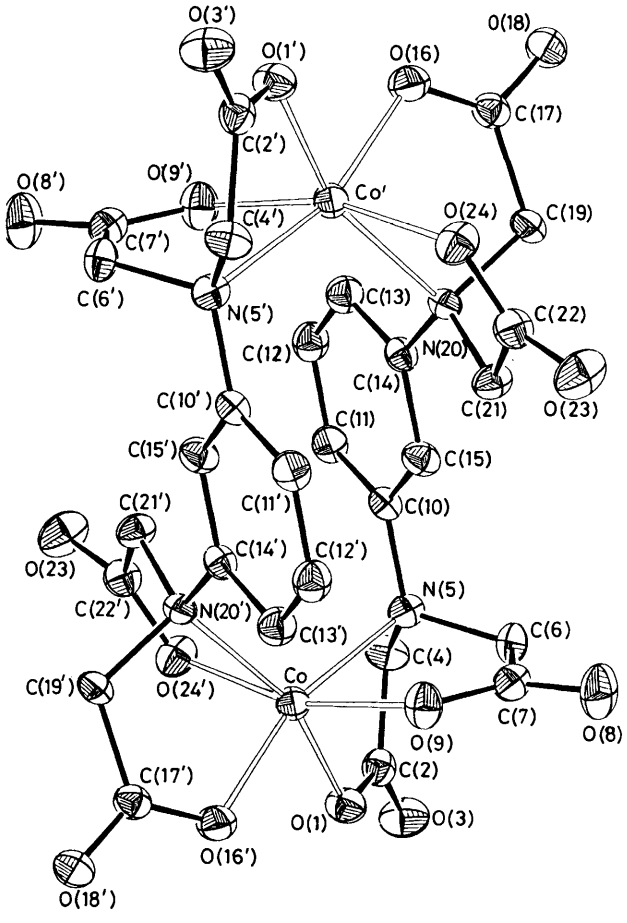

Figure 7. View of the molecular structure of the anionic complex $[Co_2(m\text{-pdta})_2]^{4-}$

Table 4. Fractional atomic co-ordinates ($\times 10^4$) with estimated standard deviations in parentheses for $Na_4[Cu_2(m\text{-pdta})_2]\cdot 18H_2O$ *

Atom	X/a	Y/b	Z/c
Cu	2 418(1)	1 989(1)	2 883(1)
Na(1)	−92(4)	5 755(4)	1 196(3)
Na(2)	3 627(4)	4 811(3)	1 231(3)
O(1)	4 591(7)	2 940(7)	2 101(5)
O(2)	6 759(7)	2 134(6)	1 669(5)
O(8)	2 221(8)	3 784(8)	5 451(7)
O(9)	1 719(7)	3 068(6)	4 031(6)
O(16′)	1 736(7)	3 194(5)	1 810(5)
O(18′)	461(7)	3 617(6)	616(6)
O(23′)	2 859(7)	−1 353(7)	1 646(6)
O(24′)	3 053(6)	664(6)	1 915(5)
N(5)	3 588(7)	1 162(7)	3 947(6)
N(20′)	274(8)	858(7)	2 819(6)
C(3)	5 504(14)	2 123(10)	2 253(8)
C(4)	5 004(9)	976(9)	3 193(8)
C(6)	3 656(10)	2 184(9)	4 641(8)
C(7)	2 433(12)	3 075(10)	4 707(10)
C(10)	2 868(10)	−23(10)	4 656(8)
C(11)	3 312(10)	−1 239(10)	4 449(8)
C(12)	2 577(11)	−2 297(9)	5 160(9)
C(13)	1 434(11)	−2 179(9)	6 055(9)
C(14)	958(10)	−958(10)	6 252(8)
C(15)	1 688(10)	129(9)	5 546(8)
C(17′)	814(10)	2 891(10)	1 347(9)
C(19′)	155(9)	1 558(9)	1 728(8)
C(21′)	818(10)	−441(9)	2 768(8)
C(22′)	2 370(10)	−360(13)	2 044(8)
OW(1)	2 282(6)	6 619(6)	577(5)
OW(2)	3 180(7)	6 063(7)	2 877(5)
OW(3)	−2 338(7)	4 651(7)	1 941(6)
OW(4)	−1 303(9)	7 444(8)	2 079(7)
OW(5)	5 877(6)	5 845(6)	595(5)
OW(6)	4 393(7)	1 461(6)	9 613(6)
OW(7)	325(8)	5 312(7)	3 285(7)
OW(8)	2 419(10)	393(8)	8 859(9)
OW(9)	4 499(9)	4 807(10)	6 249(7)

* Primed atoms are from the second ligand.

The asymmetric unit is formed by one metal atom and one whole ligand *m*-pdta (Figure 7). The whole anion has a crystallographically imposed C_i symmetry that relates both metals, and consequently both *m*-pdta ligands.

The cobalt atoms have distorted octahedral co-ordination with the two nitrogen atoms occupying relative *cis* positions (see Table 7). As for the related complex $[Cu_2(m\text{-pdta})_2]^{4-}$, the angle N–M–N shows a higher value [116.3(1)°] than those reported for analogous complexes containing *ortho*-substituted edta-like ligands, *i.e.* 79.96(7)° for $[Co(o\text{-pdta})]^{2-}$ or 84.3(1)° for $[Co(edta)]^{2-}$.[1] This circumstance is probably due to the stronger geometric constraints existing in the latter complexes that force both nitrogens to be co-ordinated to the same metal atom. The two triangular faces formed by the three donor atoms (ONO) of each iminodiacetate group make a dihedral angle of 26.9(1)°, maintaining the cobalt atom 1.293(1) Å apart from these planes. This peculiar interplanar angle is larger than the value observed for $[Co(o\text{-pdta})]^{2-}$ and is fundamentally the reason for the distortion observed for the idealized octahedral cobalt environment.

The Co–O bond distances [av. 2.049(2) Å] compare well with the separations previously reported in polyaminocarboxylate transition-metal complexes (range 1.89—2.08 Å).[1,3,4] However, the Co–N bond distances observed in $[Co_2(m\text{-pdta})_2]^{4-}$ are markedly longer than those determined for the related mononuclear compounds $[Co(o\text{-pdta})]^{2-}$ (2.184 Å) and $[Co(edta)]^{2-}$ (2.160 Å).[1]

The planes of the 'glycine' chelate rings M–O–C–C–N–M have been calculated and classified according to Hoard's proposal.[43] Rings N(5)–C(4)–C(2)–O(1) and N(20)–C(19)–C(17)–O(16) are of type G (more nearly parallel to the NMN plane), and rings N(5)–C(6)–C(7)–O(9) and N(20)–C(21)–C(22)–O(24) are of type R (more nearly perpendicular to the NMN plane).

Within the *m*-pdta ligand the different C–O bond distances for the carboxylic groups are noteworthy, with shorter distances for terminal oxygen [av. 1.236(2) Å] and longer for co-ordinated oxygen atoms [av. 1.270(2) Å]. Probably the electronic release from oxygen to the metal centre upon co-ordination creates a lower electronic availability for an additional π-carbon–oxygen interaction.

Both crystallographically independent sodium ions are five-co-ordinated involving interactions with oxygen atoms from carboxylate groups and water of crystallization [Figure 9(*a*)]. Nevertheless, two different environments are observed: Na(1) is bonded to four carboxylate oxygens [O(1), O(3), O(16), and O(18)] and to a water molecule O(33); on the other side, Na(2) is attached to two carboxylate oxygens [O(8) and O(18)] and three water molecules [O(30), O(31), and O(32)]. Interestingly, while for Na(2) all the Na–O bond distances are quite similar [within the range 2.342—2.396(2) Å], Na(1) has two longer distances to O(1) and O(16) [2.452(2) Å]. Probably these longer Na–O distances are due to the weaker donor character of these two oxygens which are also bonded to the cobalt centre. Another bridging atom is O(18), but this oxygen connects asymmetrically [2.299(2) and 2.396(2) Å] both sodium ions.

The co-ordination of Na(2) may be described as a distorted square-base pyramid, with O(8), O(30), O(31), and O(32) forming the base and O(18) in the apical position. The atom Na(2) is out of the basal plane by 0.108(1) Å. On the other hand, the presence in the co-ordination sphere of Na(1) of four carboxylic oxygen atoms, which are simultaneously linked to atoms of the anions, results in a more distorted co-ordination sphere for this metal, being intermediate between a trigonal bipyramid and a square-based pyramid. Although this type of environment for Na^+ is not very common, a similar situation has been reported for the complex $Na_2(ATP)\cdot 3H_2O$ (ATP = adenosine–triphosphate),[44] where one of the three independent Na^+ is bonded to five oxygen atoms of phosphate groups.

$Na_4[Ni_2(2,6\text{-pydta})_2]\cdot 8H_2O$. Crystals of the compound consist of sodium cations, binuclear nickel anions, and water of crystallization. The whole complex anion has crystallographic C_2 symmetry. The anion structure is similar to those of $[Cu_2(m\text{-pdta})_2]^{4-}$ and $[Co_2(m\text{-pdta})_2]^{4-}$. The asymmetric unit (Figure 8) is similar to that found in the copper complex (Figure 5).

The geometry around the nickel atom can be described essentially as a distorted octahedron with the nitrogen atoms occupying relative *cis* positions (Tables 8 and 9). The angle N(5)–Ni–N(20′) shows a higher value [115.6(2)°] than those reported for analogous *ortho*-substituted edta-like metal complexes.[1,3,4]

In the equatorial plane the co-ordination bond lengths vary for Ni–O bonds from 2.010(4) to 2.051(4) Å, while the Ni–N bond length is 2.215(4) Å (Table 9). The values are similar to those found in the cobalt compound. The Ni–O(1) bond length is 2.022(4) Å while the axial Ni–N(20′) bond distance is 2.237(4) Å. The angle O(1)–Ni–N(20′) between the axial bonds is 162.5(1)°. The angles O(16′)–Ni–N(20′) and O(24′)–Ni–N(20′) are 81.1(2) and 77.4(2)° respectively, while O(9)–Ni–N(20′) and N(5)–Ni–N(20′) are 90.0(2) and 115.6(2)° respectively. The pyridine nitrogens are not bonded to metal centres because of their positions in the aromatic rings (Figure 8).

The C–O bond distances observed for the carboxylic groups are between 1.232(6) and 1.270(6) Å.

Both crystallographically independent sodium cations are

Table 5. Selected bond distances (Å), angles (°), torsion angles (°), and planes for $Na_4[Cu_2(m\text{-pdta})_2]\cdot 18H_2O$ with estimated standard deviations (e.s.d.s) in parentheses *

(*a*) Co-ordination sphere of copper

Cu–O(1)	2.293(7)	Cu–O(24′)	1.969(7)
Cu–O(9)	1.936(7)	Cu–N(5)	2.075(8)
Cu–O(16′)	1.938(7)	Cu–N(20′)	2.509(8)
O(1)–Cu–O(9)	97.5(3)	O(1)–Cu–N(20′)	154.2(2)
O(1)–Cu–O(16′)	88.8(3)	O(9)–Cu–N(5)	84.2(3)
O(1)–Cu–O(24′)	87.8(3)	O(9)–Cu–N(20)	104.1(3)
O(9)–Cu–O(16′)	90.1(3)	O(16′)–Cu–N(5)	162.2(3)
O(9)–Cu–O(24′)	171.0(3)	O(16′)–Cu–N(20′)	77.3(3)
O(16′)–Cu–O(24′)	97.3(3)	O(24′)–Cu–N(5)	90.2(3)
O(1)–Cu–N(5)	75.4(3)	O(24′)–Cu–N(20′)	72.8(3)
		N(5)–Cu–N(20′)	120.4(3)

(*b*) In the *m*-pdta ligand

O(1)–C(3)	1.265(14)	N(5)–C(4)	1.484(11)
O(2)–C(3)	1.255(14)	N(5)–C(6)	1.503(13)
O(8)–C(7)	1.253(15)	N(5)–C(10)	1.477(11)
O(9)–C(7)	1.249(16)	N(20)–C(19′)	1.469(12)
O(16′)–C(17′)	1.290(14)	N(20)–C(21′)	1.460(12)
O(18′)–C(17′)	1.212(13)	N(20′)–C(14^{III})	1.433(12)
O(23′)–C(22′)	1.257(15)		
O(24′)–C(22′)	1.257(15)		
O(1)–C(3)–O(2)	126.4(9)	C(11)–C(10)–C(15)	120.5(9)
O(1)–C(3)–C(4)	116.4(10)	C(12)–C(13)–C(14)	119.6(9)
O(2)–C(3)–C(4)	117.1(10)	C(13)–C(14)–C(15)	119.2(9)
C(3)–C(4)–N(5)	112.5(8)	C(14)–C(15)–C(11)	119.9(9)
C(4)–N(5)–C(6)	109.5(7)	O(16′)–C(17)–O(18′)	123.3(10)
N(5)–C(6)–C(7)	110.9(8)	O(16′)–C(17′)–C(19′)	118.2(9)
N(5)–C(10)–C(11)	122.4(8)	C(17′)–C(19′)–N(20′)	116.6(8)
N(5)–C(10)–C(15)	117.1(9)	O(23′)–C(22′)–O(24′)	124.8(10)
C(6)–C(7)–O(8)	115.9(10)	C(21′)–C(22′)–O(23′)	116.5(11)
C(6)–C(7)–O(9)	119.2(10)	C(11)–C(12)–C(13)	122.3(10)
C(6)–N(5)–C(10)	112.2(7)		
O(8)–C(7)–O(9)	124.9(11)		
C(10)–C(11)–C(12)	118.5(9)		

(*c*) Co-ordination sphere of the sodium

Na(1)–O(18′)	2.477(8)	Na(2)–O(1)	2.395(8)
Na(1)–O(18^{I})	2.371(9)	Na(2)–O(16′)	2.450(7)
Na(1)–OW(1)	2.428(7)	Na(2)–OW(1)	2.456(7)
Na(1)–OW(3)	2.420(8)	Na(2)–OW(2)	2.547(8)
Na(1)–OW(4)	2.363(9)	Na(2)–OW(5)	2.389(7)
Na(1)–OW(7)	2.712(9)	Na(2)–OW(5^{II})	2.398(8)

Torsion angles

O(9)–Cu–O(1)–C(3)	116.5(7)	N(5)–Cu–O(1)–C(3)	34.5(7)
O(16′)–Cu–O(1)–C(3)	−153.6(6)	N(20′)–Cu–O(1)–C(3)	−96.9(9)
O(24′)–Cu–O(1)–C(3)	−56.2(7)	N(5)–Cu–O(9)–C(7)	16.7(7)
O(1)–Cu–O(9)–C(7)	−57.7(8)	N(20′)–Cu–O(9)–C(7)	136.7(7)
O(16′)–Cu–O(9)–C(7)	−146.4(8)	N(5)–Cu–O(16′)–C(17′)	169.9(9)
O(1)–Cu–O(16′)–C(17′)	143.4(8)	N(20′)–Cu–O(16′)–C(17′)	−14.7(7)
O(9)–Cu–O(16′)–C(17′)	−119.2(8)	N(5)–Cu–O(24′)–C(22′)	−93.3(8)
O(24′)–Cu–O(16′)–C(17′)	55.8(8)	N(20′)–Cu–O(24′)–C(22′)	−28.6(8)
O(1)–Cu–O(24′)–C(22′)	168.7(8)		
O(16′)–Cu–O(24′)–C(22′)	−102.8(8)		

Planes with deviations (Å)

Plane	
1	O(9) −0.20, O(16′) 0.17, O(24′) −0.16, N(5) 0.24, N(20′) −2.31, O(1) 2.19, Cu −0.08
2	Cu 0.01, O(9) −0.12, C(6) 0.26, C(7) 0.08, N(5) −0.19
3	Cu 0.01, O(1) −0.22, C(3) 0.26, C(4) 0.40, N(5) −0.34

Angles (°) between planes

1–2	14.4(2)	2–3	98.5(2)
1–3	99.4(2)		

* Primed atoms are for the second ligand, and atoms with roman numeral superscripts are related to those of the asymmetric unit by the transformations: I $x, -y+1, -z$; II $-x+1, -y+1, -z$; III $-x, -y, 1-z$.

Table 6. Final atomic co-ordinates ($\times 10^4$) for the non-hydrogen atoms of the complex $Na_4[Co_2(m\text{-pdta})_2]\cdot 10H_2O$

Atom	X/a	Y/b	Z/c
Co	2 332(1)	1 392(1)	2 577(1)
Na(1)	5 148(1)	2 106(1)	4 909(1)
Na(2)	3 052(1)	2 177(1)	7 027(1)
O(1)	2 954(2)	2 949(2)	3 916(1)
O(3)	3 346(2)	5 375(2)	4 520(1)
O(8)	−2 272(2)	403(2)	2 686(2)
O(9)	70(2)	227(2)	2 578(1)
O(16)	−3 452(2)	−76(2)	−3 444(1)
O(18)	−4 777(2)	1 607(2)	−3 433(1)
O(23)	−5 335(2)	−3 247(2)	−861(1)
O(24)	−4 281(2)	−2 732(2)	−2 161(1)
N(5)	1 042(2)	3 128(2)	2 073(1)
N(20)	−2 547(2)	186(2)	−1 268(1)
C(2)	2 897(3)	4 301(2)	3 802(2)
C(4)	2 215(3)	4 585(2)	2 692(2)
C(6)	−386(3)	2 654(2)	2 462(2)
C(7)	−906(3)	964(2)	2 582(2)
C(10)	633(2)	2 998(2)	961(2)
C(11)	1 480(3)	4 022(2)	429(2)
C(12)	1 016(3)	3 753(2)	−651(2)
C(13)	−283(3)	2 494(2)	−1 216(2)
C(14)	−1 131(2)	1 471(2)	−684(2)
C(15)	−673(3)	1 733(2)	388(2)
C(17)	−4 018(3)	795(2)	−2 989(2)
C(19)	−3 833(3)	790(3)	−1 841(2)
C(21)	−3 192(3)	−905(2)	−610(2)
C(22)	−4 393(3)	−2 411(2)	−1 261(2)
O(30)	4 331(3)	3 577(3)	8 691(2)
O(31)	3 389(3)	4 608(3)	6 508(2)
O(32)	1 508(4)	1 160(5)	5 263(2)
O(33)	7 416(3)	1 830(4)	4 523(3)
O(34)*	−137(11)	5 406(10)	4 550(6)
O(35)*	123(18)	3 692(16)	6 336(11)

* O(34) and O(35) represent two positions assigned to a disordered lattice water molecule. These two atoms were refined isotropically with occupancy factors 0.65 and 0.35 respectively.

five-co-ordinated (similarly to cobalt compound) involving interactions with oxygen atoms from carboxylate groups and water molecules [Figure 9(*b*)]. Two different environments are observed; Na(2) is bonded to four carboxylate oxygens, O(1), O(3), O(23), and O(24), and one water molecule, O(27) (see Table 9); Na(1) is attached to two carboxylate oxygens, O(3) and O(18), and three water molecules, O(25), O(26), and O(28). For Na(1) all Na–O bonds are similar [within range 2.319—2.399(5) Å]. For Na(2) there are two longer distances to O(1) and O(24) [2.420(4) and 2.460(5) Å respectively].

According to the bond distances and angles given in Table 9 the co-ordination of Na(1) may be described as a distorted square-based pyramid, with O(18), O(25), O(26), and O(28) forming the base and O(3) in the apical position. On the other hand, the co-ordination of Na(2) is intermediate between a trigonal bipyramid and a square-based pyramid. The molecular packing is shown in Figure 10.

Thermal, Spectroscopic, and Magnetic Studies.—The thermograms performed between 30 and 700 °C on samples of powdered single crystals of the compounds show several stages in the thermal decomposition.

For the complex $Na_4[Cu_2(m\text{-pdta})_2]\cdot 18H_2O$ the mass losses correspond in the first stage to $13H_2O$ (45—80 °C; theoretical loss 19.24%, experimental loss 19.51%), in the second stage to $2H_2O$ (82—111 °C; theoretical loss 3.67%, experimental loss 3.89%), and in the third stage to $3H_2O$ (111—200 °C; theoretical loss 5.71%, experimental loss 5.61%). Decomposition begins

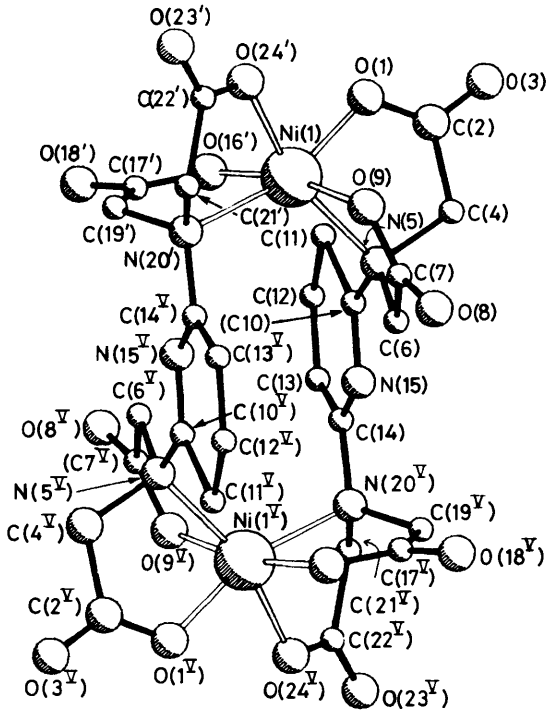

Figure 8. Molecular structure of the anionic complex $[Ni_2(2,6\text{-pydta})_2]^{4-}$ with the atomic numbering scheme included in Table 8. Primed atoms around Ni(1) belong to a different ligand unit. Atoms with superscripts V are related by the transformation $-x, -y + 1, -z$

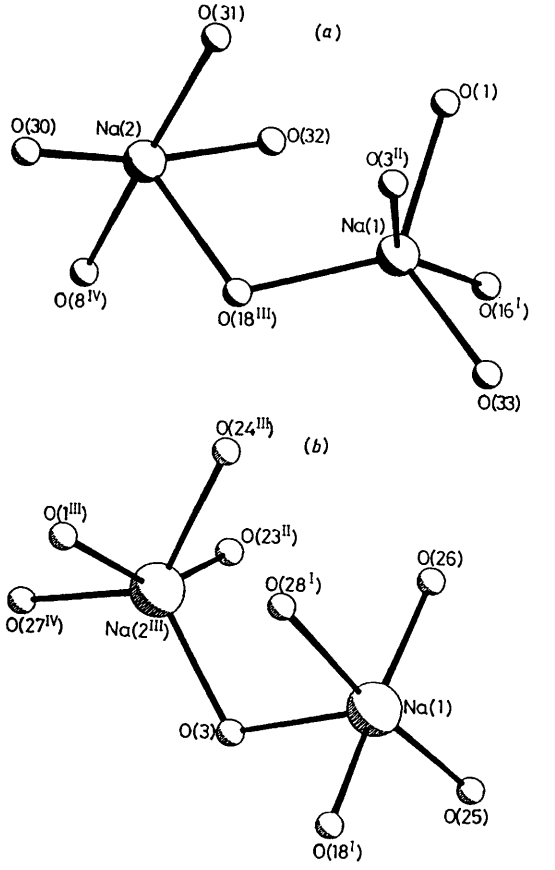

Figure 9. Co-ordination geometry of the sodium atoms in (*a*) $Na_4[Co_2(m\text{-pdta})_2]\cdot 10H_2O$ and (*b*) $Na_4[Ni_2(2.6\text{-pydta})_2]\cdot 8H_2O$ with the atomic numbering schemes shown in Tables 7 and 9 respectively

Table 7. Selected bond distances (Å) angles (°), torsion angles (°), and planes for $Na_4[Co_2(m\text{-pdta})_2]\cdot 10H_2O$ with e.s.d.s in parentheses *

(*a*) Co-ordination sphere of cobalt

Co–O(1)	2.072(2)	Co–O(16^{I})	2.037(2)
Co–O(9)	2.017(2)	Co–O(24^{I})	2.069(2)
Co–N(5)	2.281(2)	Co–N(20^{I})	2.297(2)
O(1)–Co–O(9)	97.7(1)	O(9)–Co–N(20^{I})	99.0(1)
O(1)–Co–N(5)	75.9(1)	N(5)–Co–O(16^{I})	163.1(1)
O(1)–Co–O(16^{I})	88.5(1)	N(5)–Co–O(24^{I})	88.5(1)
O(1)–Co–O(24^{I})	90.5(1)	N(5)–Co–N(20^{I})	116.3(1)
O(1)–Co–O(20^{I})	160.9(1)	O(16^{I})–Co–O(24^{I})	98.3(1)
O(9)–Co–N(5)	79.0(1)	O(16^{I})–Co–N(20^{I})	80.5(1)
O(9)–Co–O(16^{I})	97.0(1)	O(24^{I})–Co–N(20^{I})	75.9(1)
O(9)–Co–O(24^{I})	162.8(1)		

(*b*) In the *m*-pdta ligand

C(2)–O(1)	1.276(3)	C(17)–O(16)	1.274(3)
C(2)–O(3)	1.231(3)	C(17)–O(18)	1.239(3)
C(2)–C(4)	1.535(4)	C(17)–C(19)	1.514(4)
C(7)–O(9)	1.264(3)	C(22)–O(24)	1.267(3)
C(7)–O(8)	1.243(3)	C(22)–O(23)	1.232(3)
C(7)–C(6)	1.517(3)	C(22)–C(21)	1.528(2)
N(5)–C(4)	1.477(2)	N(20)–C(19)	1.495(3)
N(5)–C(6)	1.481(3)	N(20)–C(21)	1.474(3)
N(5)–C(10)	1.436(3)	N(20)–C(14)	1.459(2)
O(1)–C(2)–O(3)	124.3(2)	O(16)–C(17)–O(18)	124.3(2)
O(1)–C(2)–C(4)	117.1(2)	O(16)–C(17)–C(19)	118.5(2)
O(3)–C(2)–C(4)	118.6(2)	O(18)–C(17)–C(19)	117.1(2)
O(9)–C(7)–O(8)	124.5(2)	O(24)–C(22)–O(23)	125.1(2)
O(9)–C(7)–C(6)	118.4(3)	O(24)–C(22)–C(21)	116.6(2)
O(8)–C(7)–C(6)	117.1(3)	O(23)–C(22)–C(21)	118.2(2)
C(4)–N(5)–C(6)	110.4(2)	C(19)–N(20)–C(21)	109.5(2)
C(4)–N(5)–C(10)	117.9(2)	C(19)–N(20)–C(14)	109.6(2)
C(6)–N(5)–C(10)	113.2(2)	C(21)–N(20)–C(14)	113.2(2)
N(5)–C(4)–C(2)	108.9(2)	N(20)–C(19)–C(17)	115.6(2)
N(5)–C(6)–C(7)	113.5(2)	N(20)–C(21)–C(22)	111.5(2)

(*c*) Co-ordination sphere of the sodium

Na(1)–O(1)	2.453(2)	Na(2)–O(8^{IV})	2.355(2)
Na(1)–O(3^{II})	2.277(2)	Na(2)–O(18^{III})	2.396(2)
Na(1)–O(16^{I})	2.452(2)	Na(2)–O(30)	2.342(3)
Na(1)–O(18^{III})	2.299(2)	Na(2)–O(31)	2.342(3)
Na(1)–O(33)	2.328(4)	Na(2)–O(32)	2.390(3)
O(1)–Na(1)–O(3^{II})	88.8(1)	O(8^{IV})–Na(2)–O(18^{III})	85.1(1)
O(1)–Na(1)–O(16^{I})	71.5(1)	O(8^{IV})–Na(2)–O(30)	104.0(1)
O(1)–Na(1)–O(18^{III})	119.1(1)	O(8^{IV})–Na(2)–O(31)	169.8(1)
O(1)–Na(1)–O(33)	131.3(1)	O(8^{IV})–Na(2)–O(32)	85.1(1)
O(3^{II})–Na(1)–O(16^{I})	148.3(1)	O(18^{III})–Na(2)–O(30)	100.0(1)
O(3^{II})–Na(1)–O(18^{III})	92.4(1)	O(18^{III})–Na(2)–O(31)	99.3(1)
O(3^{II})–Na(1)–O(33)	85.8(1)	O(18^{III})–Na(2)–O(32)	86.0(1)
O(16^{I})–Na(1)–O(18^{III})	118.6(1)	O(30)–Na(2)–O(31)	84.4(1)
O(16^{I})–Na(1)–O(33)	89.0(1)	O(30)–Na(2)–O(32)	169.5(1)
O(18^{III})–Na(1)–O(33)	109.5(1)	O(31)–Na(2)–O(32)	86.0(1)

Torsion angles

O(24^{I})–Co–N(5)–C(4)	−54.87(1)	O(24^{I})–Co–N(5)–C(6)	−169.55(1)
O(16^{I})–Co–N(5)–C(4)	59.49(4)	O(16^{I})–Co–N(5)–C(10)	−175.47(3)
O(9)–Co–N(5)–C(4)	136.98(1)		

Planes

1 Co −0.06, N(5) −0.11, O(1) 0.24, O(16^{I}) −0.17, N(20^{I}) 0.19
2 Co 0.45, O(24^{I}) 0.21, O(16^{I}) −0.24, O(9) 0.24, N(5) −0.26
3 Co −0.02, N(20^{I}) −0.24, O(24^{I}) 0.29, O(1) −0.23, O(9) 0.22

Angles (°) between planes

1–2	95.20(5)	2–3	77.71(4)
1–3	87.31(5)		

* Atoms with roman numeral superscripts are related to those of the asymmetric unit by the transformations: I $-x, -y, -z$; II $1-x, 1-y, 1-z$; III $1+x, y, 1+z$; IV, $-x, -y, 1-z$.

Table 8. Fractional atomic co-ordinates ($\times 10^4$) with e.s.d.s in parentheses for $Na_4[Ni_2(2,6\text{-pydta})_2]\cdot 8H_2O$

Atom	X/a	Y/b	Z/c
Ni	1 376(1)	7 360(2)	2 516(1)
O(1)	101(4)	8 449(4)	3 408(2)
C(2)	−800(5)	8 989(5)	2 966(3)
O(3)	−1 631(4)	9 721(4)	3 401(3)
C(4)	−845(5)	8 808(5)	1 795(3)
N(5)	−237(4)	7 504(4)	1 230(3)
C(6)	785(5)	8 128(5)	518(3)
C(7)	2 307(5)	9 358(5)	1 183(3)
O(8)	3 146(4)	10 312(4)	757(3)
O(9)	2 659(4)	9 344(4)	2 123(3)
C(10)	−1 542(5)	6 046(5)	682(3)
C(11)	−2 538(5)	5 281(5)	1 529(3)
C(12)	−3 806(5)	3 973(5)	699(4)
C(13)	−4 056(5)	3 447(5)	−400(3)
C(14)	−2 967(5)	4 297(5)	−891(3)
N(15)	−1 726(4)	5 579(4)	−358(3)
O(16)	195(4)	5 149(4)	2 606(3)
C(17)	885(5)	4 107(5)	2 514(3)
O(18)	3 040(4)	2 731(4)	2 588(3)
C(19)	2 559(5)	4 606(5)	2 360(3)
N(20)	3 053(4)	6 083(4)	2 003(3)
C(21)	4 531(5)	7 253(5)	2 661(3)
C(22)	4 264(5)	7 905(5)	3 773(3)
O(23)	5 358(4)	8 336(5)	4 517(3)
O(24)	2 917(4)	7 968(4)	3 868(2)
Na(1)	−2 182(2)	11 962(3)	3 001(2)
Na(2)	2 102(2)	10 153(3)	4 909(2)
O(25)	−3 648(4)	10 590(5)	1 331(3)
O(26)	−4 623(4)	11 627(5)	3 502(3)
O(27)	1 831(6)	2 445(6)	4 470(5)
O(28)	−969(7)	3 394(6)	4 798(4)

above 210 °C. In accord with the structure of this compound described above, it is expected that the $15H_2O$ lost in the first and second stages are those molecules weakly bonded by hydrogen bridges, as well as those singly-co-ordinated to the sodium cations. The $3H_2O$ lost in the third stage may correspond to the bridging two-co-ordinated water molecules and those which act as a bridge between carboxylate groups and sodium atoms.

For the complex $Na_4[Co_2(m\text{-pdta})_2]\cdot 10H_2O$ the first and second weight losses occur between 30 and 200 °C corresponding to four water molecules (theoretical loss 6.78%, experimental loss 7.75%). The loss of the other six water molecules occurs in the third stage where the decomposition of the compound begins above 250 °C. It is expected that the water molecules lost in the first and second stages of decomposition are those molecules of crystallization. The six remaining molecules co-ordinated to the sodium cations are removed together when decomposition occurs above 250 °C.

In $Na_4[Ni_2(2,6\text{-pydta})_2]\cdot 8H_2O$ the water molecules are removed at 200 °C, thermal decomposition beginning at 320 °C.

According to the initial temperature of decomposition of the anhydrous complexes, the order of thermal stability is $Cu^{II} < Ni^{II} < Co^{II}$. The lower stability of the copper complex is due to its higher distortion with respect to the nickel and cobalt complexes.

The i.r. spectra of the three complexes show bands at 2 880—2 940 cm^{-1} which are attributed to CH stretching frequencies of the CH_2 of the iminodiacetate groups.[4,5] The i.r. spectrum of the copper complex shows a band at 3 460 cm^{-1} corresponding to the stretching vibrations of OH groups of non-co-ordinated water molecules involved in hydrogen bonding. The spectrum of the cobalt complex presents one broad band between 3 500 and 3 360 cm^{-1} which is attributed to stretching vibrations of

Table 9. Selected bond distances (Å), angles (°), torsion angles (°), and planes for $Na_4[Ni_2(2,6\text{-pydta})_2]\cdot 8H_2O$ with e.s.d.s in parentheses

(*a*) Co-ordination sphere of nickel

Ni–O(1)	2.022(4)	Ni–O(16′)	2.010(4)
Ni–O(9)	2.051(4)	Ni–O(24′)	2.032(4)
Ni–N(5)	2.215(4)	Ni–N(20′)	2.237(4)
O(1)–Ni–O(9)	97.6(2)	O(9)–Ni–N(20′)	90.0(2)
O(1)–Ni–N(5)	81.6(2)	N(5)–Ni–O(16′)	99.2(2)
O(1)–Ni–O(16′)	93.2(2)	N(5)–Ni–O(24′)	162.1(2)
O(1)–Ni–O(24′)	86.7(2)	N(5)–Ni–N(20′)	115.6(2)
O(1)–Ni–N(20′)	162.5(1)	O(16′)–Ni–O(24′)	94.9(2)
O(9)–Ni–N(5)	76.9(2)	O(16′)–Ni–N(20′)	81.1(2)
O(9)–Ni–O(16′)	167.7(2)	O(24′)–Ni–N(20′)	77.4(2)
O(9)–Ni–O(24′)	91.4(2)		

(*b*) In the 2,6-pydta ligand

C(2)–O(1)	1.249(6)	C(17′)–O(16′)	1.268(7)
C(2)–O(3)	1.240(6)	C(17′)–O(18′)	1.232(6)
C(2)–C(4)	1.524(6)	C(17′)–C(19′)	1.516(6)
N(5)–C(4)	1.510(6)	C(22′)–C(21′)	1.522(6)
N(5)–C(6)	1.489(6)	C(22′)–O(23′)	1.239(5)
N(5)–C(10)	1.458(5)	C(22′)–O(24′)	1.270(6)
C(7)–C(6)	1.527(5)	N(20′)–C(14′)	1.424(6)
C(7)–O(8)	1.261(6)	N(20′)–C(19′)	1.487(6)
C(7)–O(9)	1.269(6)	N(20′)–C(21′)	1.481(5)
O(1)–C(2)–O(3)	126.0(4)	O(16′)–C(17′)–O(18′)	124.1(5)
O(1)–C(2)–C(4)	117.8(4)	O(16′)–C(17′)–C(19′)	118.2(5)
O(3)–C(2)–C(4)	116.2(5)	O(18′)–C(17′)–C(19′)	117.6(5)
O(9)–C(7)–O(8)	124.1(5)	O(24′)–C(22′)–O(23′)	124.6(4)
O(9)–C(7)–C(6)	118.1(4)	O(24′)–C(22′)–C(21′)	116.8(4)
O(8)–C(7)–C(6)	117.7(4)	O(23′)–C(22′)–C(21′)	118.6(4)
C(4)–N(5)–C(6)	109.4(4)	C(19′)–N(20′)–C(21′)	110.9(4)
C(4)–N(5)–C(10)	109.1(4)	N(20′)–C(19′)–C(17′)	114.3(4)
C(6)–N(5)–C(10)	133.3(3)	N(20′)–C(21′)–C(22′)	109.2(4)
N(5)–C(4)–C(2)	114.1(4)		
N(5)–C(6)–C(7)	108.9(3)		

(*c*) Co-ordination sphere of the sodium

Na(1)–O(18^{I})	2.339(5)	Na(2^{III})–O(1^{III})	2.420(4)
Na(1)–O(28^{I})	2.399(5)	Na(2^{III})–O(3)	2.314(4)
Na(1)–O(3)	2.393(5)	Na(2^{III})–O(23^{II})	2.269(4)
Na(1)–O(25)	2.319(4)	Na(2^{III})–O(24^{III})	2.460(5)
Na(1)–O(26)	2.351(5)	Na(2^{III})–O(27^{IV})	2.360(7)
O(18^{I})–Na(1)–O(28^{I})	86.6(2)	O(3)–Na(2^{III})–O(27^{IV})	109.6(2)
O(26)–Na(1)–O(28^{I})	89.4(2)	O(3)–Na(2^{III})–O(23^{II})	93.0(2)
O(26)–Na(1)–O(18^{I})	171.0(2)	O(3)–Na(2^{III})–O(24^{III})	121.8(2)
O(25)–Na(1)–O(28^{I})	172.7(2)	O(3)–Na(2^{III})–O(1^{III})	120.0(2)
O(25)–Na(1)–O(18^{I})	100.4(2)	O(23^{II})–Na(2^{III})–O(27^{IV})	85.5(2)
O(25)–Na(1)–O(26)	83.4(2)	O(24^{III})–Na(2^{III})–O(27^{IV})	128.5(2)
O(3)–Na(1)–O(28^{I})	84.2(2)	O(24^{III})–Na(2^{III})–O(23^{II})	88.5(2)
O(3)–Na(1)–O(18^{I})	87.5(2)	O(1^{III})–Na(2^{III})–O(27^{IV})	88.7(2)
O(3)–Na(1)–O(26)	100.2(2)	O(1^{III})–Na(2^{III})–O(23^{II})	146.4(2)
O(3)–Na(1)–O(25)	98.1(2)	O(1^{III})–Na(2^{III})–O(24^{III})	69.5(1)

Torsion angles

O(16)–Ni–O(24)–C(22)	103.3(4)	O(24)–Ni–N(20)–C(19)	79.7(3)
O(9)–Ni–O(24)–C(22)	−66.2(4)	O(1)–Ni–N(20)–C(19)	54.7(8)
N(5)–Ni–O(20)–C(21)	131.6(3)		

Planes

1 N(5) 0.00, O(9) 0.00, O(1) 0.00, Ni 1.27
2 N(20′) 0.00, O(24′) 0.00, O(16′) 0.00, Ni −1.29
3 N(5) 0.16, C(4) −0.21, C(2) 0.01, O(1) 0.10, Ni −0.05

Angles (°) between planes

1–2	25.6(2)	2–3	65.8(2)
1–3	59.1(1)		

* Atoms with roman numeral superscripts are related to those of the asymmetric unit by the transformations: I $x, y + 1, z$; II $x - 1, y, z$; III $-x, y + 2, -z + 1$; IV $-x, -y + 1, -z + 1$; V $-x, -y + 1, -z$.

Figure 10. Molecular packing for the compound $Na_4[Ni_2(2,6\text{-pydta})_2]\cdot 8H_2O$

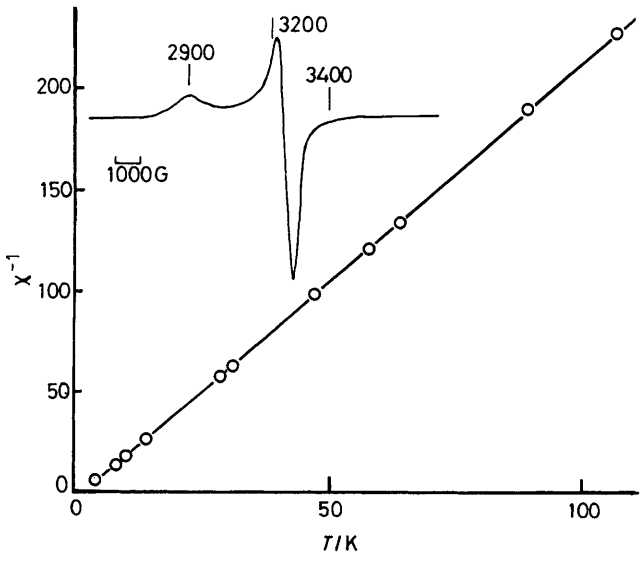

Figure 11. Inverse molar susceptibility as a function of temperature (K) and e.s.r. spectrum for the complex $Na_4[Cu_2(m\text{-pdta})_2]\cdot 18H_2O$

the OH group of water, both reticular and co-ordinated to the sodium. The spectrum of the nickel complex shows one symmetrical band at 3 400 cm^{-1} which is assigned to stretching vibrations of the OH groups of the water co-ordinated to the sodium. The assignments of the bands observed are in accordance with the type of bonds for the water molecules found in the respective structures. The deformation vibrations of the water are overlapped by the broad band between 1 550 and 1 650 cm^{-1} which corresponds to CO_2^- groups co-ordinated to the metal. The width of this band established the difference between the closest carboxylate groups bonded to the metal and the carboxylate groups bonded axially to the metal.[45]

The visible electronic spectrum of the copper complex shows a broad band at 750 nm and another much more intense band at 385 nm. These bands coincide with those found in aqueous solution for the complex *m*-pdta–Cu^{II} [39] in a 1:1 ratio and at pH 5.5. The broad band at 750 nm is the ligand-field band for distorted octahedral copper(II) complexes.[46] The band with most energy and intensity at 385 nm is a ligand to metal charge transfer,[39,46] fundamentally comprised of $\sigma \longrightarrow \sigma^*$ transitions from the Cu–N bond to the empty $x^2 - y^2$ orbital.[46]

The diffuse reflectance spectrum of the cobalt(II) complex shows bands at 385, 580, and 800 nm. The band at 385 nm is assigned to ligand to metal charge transfer similarly to the copper complex. Other bands at 580 and 800 nm correspond to ligand-field transitions of the distorted octahedral cobalt complex (Figure 7) as described above and the assignment is complicated due to the lower symmetry compared with O_h.[46] The electronic spectrum in aqueous solution shows bands at 466 (ε 67.05 $dm^3\ mol^{-1}\ cm^{-1}$), 494 (73.75), 534 (118.45), and 620 nm (5.34). The bands at 466 and 494 nm are attributed to ligand to metal charge transfer. The changes in the position of the bands with respect to solid-state spectrum are due to the mixture of monomer and dimer species which exists in aqueous solution in accordance with the species distribution diagrams.[21] Thus for the concentration of the solution used to obtain the spectrum (1×10^{-3} mol dm^{-3}) there is 50.7% monomer and 40%

dimer. Therefore the bands at 534 and 620 nm fundamentally correspond to $^4T_{1g}(P) \longrightarrow {}^4T_{1g}$ and $^4A_{2g} \longrightarrow {}^4T_{1g}$ transitions of monomeric species in accordance with the behaviour of other complexes of cobalt(II).[1]

The diffuse reflectances spectrum of the nickel(II) complex shows bands at 380 and 625 nm and a shoulder between 700 and 725 nm. The band at 380 nm is a ligand to metal charge transfer similarly to those of the cobalt and copper complexes. The bands at 625 and 700—725 nm are assigned to the $^3T_{1g} \longrightarrow {}^3A_{2g}$ transition corresponding to an octahedral nickel(II) complex.[46]

The measurement of the effective magnetic moment for $Na_4[Cu_2(m\text{-pdta})_2]\cdot 18H_2O$ at 288 K is 1.93 B.M. The study of the magnetic susceptibilities as a function of temperature in the range 4.2—288.5 K reveals a normal paramagnetic behaviour fulfilling the Curie law (Figure 11). The partial cancellation of the spins of the copper(II) ions described for a similar complex[16] is therefore not observed. In agreement with the co-ordination geometry revealed by the *X*-ray structure, the room-temperature *X*-band e.s.r. spectrum of a polycrystalline sample of the copper compound (Figure 11) shows a typical axial signal with $g_{\parallel} = 2.33$ and $g_{\perp} = 2.08$ ($g_{av.} = 2.16$). These results indicate that the ground state is predominantly $d_{x^2-y^2}$ for the Cu^{II}.[4,7] There is no appreciable change in the e.s.r. spectrum on decreasing the temperature of the sample from room temperature to 4.2 K.

For $Na_4[Co_2(m\text{-pdta})_2]\cdot 10H_2O$ the magnetic moment at 293 K is 5.01 B.M. This value is consonant with octahedral co-ordination around the cobalt(II) ion without magnetic interactions.[48]

The magnetic moment for $Na_4[Ni_2(2,6\text{-pydta})_2]\cdot 8H_2O$ at 298 K is 2.94 B.M. This result is consonant with an octahedral stereochemistry around nickel(II), in accordance with the structure described above.[48]

Acknowledgements

We thank the Computer Center of the Faculty of Science Universidad Central de Venezuela (UCV) for computer time on the Burroughs 6700, Consejo Nacional de Investigaciones Cientificas y Tecnológicas (Caracas, Grant No. 51.78.31.S1-1228), Consejo de Desarrollo Cientifico y Humanístico (UCV, Grant No. C-03.12/83), and the Education Council of the Canary Islands Government (Grant No. 86/22.04.85) for financial support.

References

1 E. F. K. McCandlish, T. K. Michael, J. A. Neal, E. C. Lingafelter, and N. J. Rose, *Inorg. Chem.*, 1978, **17**, 1383.
2 N. Nakasuka, Sh. Azuma, Ch. Katayama, M. Honda, J. Tanaka, and M. Tanaka, *Acta Crystallogr., Sect. C*, 1985, **41**, 1176.
3 Sh. Azuma, N. Nakasuka, and M. Tanaka, *Acta Crystallogr., Sect. C*, 1986, **42**, 673.
4 N. Nakasuka, Sh. Azuma, and M. Tanaka, *Acta Crystallogr., Sect. C*, 1986, **42**, 1485.
5 N. Nakasuka, M. Kunimatsu, K. Matsumura, and M. Tanaka, *Inorg. Chem.*, 1985, **24**, 10.
6 K. Matsumura, N. Nakasuka, and M. Tanaka, *Inorg. Chem.*, 1987, **26**, 1419.
7 A. Mederos, J. V. Herrera, and J. M. Felipe, *An. Quím.*, 1985, **81B**, 152; 1987, **83B**, 22.
8 A. Mederos, J. M. Felipe, M. Hernández-Padilla, F. Brito, E. Chinea, and K. Bazdikian, *J. Coord. Chem.*, 1986, **14**, 277.
9 F. Brito, A. Mederos, J. V. Herrera, S. Domínguez, and M. Hernández-Padilla, *Polyhedron*, 1988, **7**, 1187.
10 E. Uhlig and D. Herrmann, *Z. Anorg. Allg. Chem.*, 1968, **360**, 158.
11 C. Ruíz-Pérez, M. L. Rodríguez, F. V. Rodríguez-Romero, A. Mederos, P. Gili, and P. Martín-Zarza, *Acta Crystallogr., Sect. C*, in the press.
12 A. Mederos, J. M. Felipe, F. Brito, and K. Bazdikian, *J. Coord. Chem.*, 1986, **14**, 285.
13 A. Mederos, S. Domínguez, M. Hernández-Padilla, F. Brito, and E. Chinea, *Bol. Soc. Quim. Peru*, 1984, **50**, 277.
14 C. A. Bear, J. M. Waters, and T. N. Waters, *J. Chem. Soc. A*, 1970, 2494.
15 A. Mederos, F. G. Manrique, A. Medina, and G. de la Fuente, *An. Quím.*, 1983, **79B**, 377.
16 S. González García and F. J. Sánchez Santos, *An. Quím.*, 1976, **72**, 153; 1981, **77B**, 175.
17 A. Mederos, A. Rodríguez González, and B. Rodríguez Ríos, *An. Quím.*, 1973, **69**, 731.
18 A. Mederos, A. Benítez, A. Rancel, R. Guerra, F. Brito, K. Bazdikian, and J. Bruzal, *J. Coord. Chem.*, 1986, **15**, 85.
19 F. Brito and J. M. Gonçalves, Project No. 51.78.-31-51-1228, CONICIT, Caracas, 1981.
20 R. Arnek, L. G. Sillén, and O. Wahlberg, *Ark. Kemi*, 1969, **61**, 353.
21 F. Brito, A. Mederos, P. Gili, S. Domínguez, and P. Martín-Zarza, *J. Coord. Chem.*, 1988, **17**, 311.
22 F. Brito, A. Mederos, P. Gili, R. Guerra, S. Domínguez, and M. Hernández-Padilla, *J. Coord. Chem.*, 1989, **20**, 169.
23 E. Blasius and G. Olbrich, *Z. Anal. Chem.*, 1956, **151**, 81.
24 A. Mederos, J. V. Herrera, A. Benítez, and A. Rancel, *An. Quím.*, 1988, **84B**, 5.
25 F. Brito and N. Ingri, *An. Quím.*, 1960, **56B**, 165.
26 G. Biedermann and L. G. Sillén, *Ark. Kemi*, 1953, **5**, 425.
27 A. Sabatini, A. Vacca, and P. Gans, *Talanta*, 1974, **21**, 53.
28 R. N. Sylva and M. R. Davidson, *J. Chem. Soc., Dalton Trans.*, 1979, 232.
29 C. Orvig, *J. Chem. Educ.*, 1985, **62**, 84.
30 P. Jones, *Chem. Brit.*, 1981, **17**, 222.
31 J. M. Stewart, F. A. Kundell, and J. C. Baldwin, 'The *X*-RAY 76 System,' Computer Science Center, University of Maryland, College Park, Maryland, 1970.
32 N. Walker and D. Stuart, *Acta Crystallogr., Sect. A*, 1983, **39**, 158.
33 J. Fayos and Martínez Ripoll, 'HSEARCH program,' Instituto Rocosolano, Madrid, Spain, 1980.
34 'International Tables for *X*-Ray Crystallography,' Kynoch Press, Birmingham, vol. 4, 1974; present distributor D. Reidel, Dordrecht.
35 G. M. Sheldick, 'SHELX program for crystal structure determination,' University of Cambridge, 1976.
36 A. C. T. North, D. C. Phillips, and F. S. Mathews, *Acta Crystallogr., Sect. A*, 1968, 351.
37 (*a*) K. L. Rinehart, *Science*, 1982, **218**, 254; (*b*) I. Busch and R. G. Cooks, *ibid.*, p. 247.
38 A. Mederos, J. Fuentes, E. Medina, P. Martín-Barroso, and B. Rodríguez Ríos, *An. Quím.*, 1980, **76B**, 352.
39 A. Mederos, A. Rodríguez González, and B. Rodríguez Ríos, *An. Quím.*, 1973, **69**, 601.
40 A. Mederos, F. G. Manrique, J. V. Herrera, M. Alvarez-Romero, and J. M. Felipe, *An. Quím.*, 1986, **82B**, 133.
41 F. S. Stephens, *J. Chem. Soc. A*, 1969, 1723.
42 X. Solans, M. Font-Altaba, Oliva, and J. Herrera, *Acta Crystallogr., Sect. C*, 1983, **39**, 435.
43 H. E. Weakliem and J. L. Hoard, *J. Am. Chem. Soc.*, 1959, **81**, 549.
44 J. Bello, D. Hass, and H. R. Bello, *Biochemistry*, 1966, **5**, 2539.
45 K. Nakamoto, 'Infrared and Raman Spectra of Inorganic and Coordination Compounds.' 4th edn., Wiley, New York, 1986, p. 228 and 237.
46 A. B. P. Lever, 'Inorganic Electronic Spectroscopy,' 2nd edn., Elsevier, Amsterdam, 1984, chs. 5 and 6.
47 B. J. Hathaway, *Struct. Bonding (Berlin)*, 1984, **57**, 55.
48 F. A. Cotton and G. Wilkinson, 'Advanced Inorganic Chemistry,' 5th edn., Wiley, New York, 1988.

Received 1*st August* 1989; *Paper* 9/03541I